PLATINUM(II) METALLOTHIONEINS

By

JACOB BONGERS

A DISSERTATION PRESENTED TO THE GRADUATE SCHOOL
OF THE UNIVERSITY OF FLORIDA IN PARTIAL FULFILLMENT
OF THE REQUIREMENTS FOR THE DEGREE OF
DOCTOR OF PHILOSOPHY

UNIVERSITY OF FLORIDA

1989

To my parents

ACKNOWLEDGMENTS

The Plasma II was purchased with a Biomedical Research Support grant funded by the National Institutes of Health and administered by the Division of Sponsored Research, University of Florida. Partial support of this project was provided by a Milheim Foundation grant and the Division of Sponsored Research, University of Florida.

I thank David Richardson for helping me in all aspects of my work, and I appreciate his passionate interest in chemistry. John Bell deserve thanks for collaborating with us on several projects and undertaking the difficult job of isolating and purifying the protein used in this study. I also thank Joanne Lopez for her valuable technical assistance. I thank Frances Goodman for her kind assistance in operating and maintaining the instruments, and for many helpful discussions about both of our research projects. Dr. Roy King is acknowledged for his valuable assistance and I owe a special debt of gratitude to Cyndy Walton for her expert assistance in the NMR spectroscopy. My thanks go out to the faculty and students of the inorganic division for their fine spirit of cooperation.

TABLE OF CONTENTS

LIST OF TABLES

LIST OF FIGURES

Abstract of Dissertation Presented to the Graduate School of the University of Florida in Partial Fulfillment of the Requirements for the Degree of Doctor of Philosophy

PLATINUM(II) METALLOTHIONEINS

By

Jacob Bongers

May 1989

Chairman: David E. Richardson
Major Department: Chemistry

Platinum(II) adducts of the metal ion chelating protein, metallothionein (MT), were prepared and characterized by spectroscopic and other methods. ApoMT reacts with excess K_2PtCl_4 at pH 7 to form a monomeric adduct containing 6.95 ± 0.24 mol Pt/mol MT as determined by inductively coupled plasma atomic emission spectrometry (ICP-AES). Polymeric adducts containing 17 ± 2 mol Pt/mol MT are formed at pH 2. The Stokes' radius of Pt_7MT is consistent with a two-domain structure containing two independent metal-thiolate cluster regions similar to that of native MT.

Spectrophotometric and spectropolarimetric titrations of apoMT with K_2PtCl_4 at neutral pH suggest that the first three mol equiv of Pt^{2+} ions form three $Pt(cys)_4^{2-}$ units, and that the binding of the remaining four mol equiv of Pt^{2+}

ions involves formation of bridging thiolates and Pt(II)-thiolate clusters. This binding sequence was confirmed by titration of the partially platinated apoMT adducts with the thiolate assay reagent, DTNB. The biphasic kinetics of Pt(II) binding to apoMT are also consistent with this interpretation.

Reactions of Cd_7MT and native MT with K_2PtCl_4, in the presence of air, result in the liberation of three mol equiv of the originally bound metal ions and the binding of one mol equiv of Pt^{2+}. When air is excluded from the reaction, three mol equiv of metal ions are lost and four mol equiv of Pt^{2+} are bound. Pt(II) preferentially displaces metal ions from the 3-metal ß-cluster region in reactions of native MT with derivatives of the antitumor drug, cis-$Pt(NH_3)_2Cl_2$, as shown by analytical and ^1H NMR data. Binding to native MT of Pt(II) from cis-$Pt(ATMPO)_2Cl_2$, resulted in trans-labilization of the spin-labeled ATMPO amine ligand, and the analytical results suggest binding of Pt(II) to the N-terminal methionine.

Possible Pt(II)-thiolate cluster structures for Pt_7MT and mixed-metal Pt(II) metallothioneins are described. Implications for the metabolism of platinum anticancer drugs are discussed. A method for the determination of micromolar protein concentrations and the metal binding stoichiometries of metalloproteins by ICP-AES of sulfur is also described.

CHAPTER 1
INTRODUCTION

Metallothionein

Metallothioneins are low-molecular-weight cytosolic proteins with extremely high metal and sulfur contents [1-4]. These proteins occur in natural systems ranging from microorganisms to humans. Metallothionein was discovered in 1957 by Margoshes and Vallee in a search for a tissue constituent responsible for the natural accumulation of cadmium in animal tissues [5]. Although the biological role of metallothionein is not known for certain it is thought to be involved in the regulation of the essential trace elements Zn and Cu. Metallothionein also binds various heavy metals ions *in vivo* including Cd(II), Hg(II), and Pb(II), and biosynthesis of the protein is stimulated by the presence of certain of these metal ions. This interesting phenomenon suggests a role in the sequestering of toxic metal ions.

Mammalian forms of MT are single polypeptides of 61 amino acid residues with molecular weights ranging from 6500 to 7000 Daltons depending on the metallic composition. The primary structures of the three metallothioneins employed in this study are shown in Figure 1-1 [6, 7]. Most vertebrate

```
                                    1                   10
Equine Kidney MT-1A      Ac-M D P N C S C P T G G S C -
Rat Liver     MT-1       Ac-M D P N C S C S T G G S C -
Rat Liver     MT-2       Ac-M D P N C S C A T D G S C -

                  20                  30
- T C A G S C K C K E C R C T S C K K S C C S C C P -
- T C S S S C G C K N C K C T S C K K S C C S C C P -
- S C A G S C K C K Q C K C T S C K K S C C S C C P -

   40                  50                  60
- G G C A R C A Q G C V C K G A S D K C S C C A-OH
- V G C S K C A Q G C V C K G A S D K C T C C A-OH
- V G C A K C S Q G C I C K E A S D K C S C C A-OH
```

Figure 1-1. Amino acid sequences of equine kidney MT-1A [6], rat liver MT-1 [7], and rat liver MT-2 [7]. The one-letter amino acid code is: A, alanine; C, cysteine; D, aspartic acid; E, glutamic acid; G, glycine; I, isoleucine; K, lysine; M, methionine; N, asparagine; P, proline; Q, glutamine; S, serine; T, threonine; V, valine.

tissues contain two major "isoforms" of metallothionein designated MT-1 and MT-2 according to the order of elution by ion exchange chromatography. Some samples of MT-1 may be further resolved into subforms MT-1A, MT-1B, and so on. All mammalian forms of MT contain 20 cysteine residues (CH_2SH side chain) at identical positions in the sequence and an N-terminal acetylated methionine ($CH_2CH_2SCH_3$ side chain) giving a total of 21 sulfur atoms. The complete lack of residues with aromatic side chains is another unusual feature of MT.

Native MT binds a total of 7 divalent metal ions, primarily Cd^{2+} and Zn^{2+} and often contains minor amounts of Cu^{+}, Fe^{2+}, Hg^{2+}, Pb^{2+}, and other metal ions depending on the source and method of isolation. Although MT from adult tissue contains predominantly Cd^{2+} and Zn^{2+}, MT from fetal tissue generally contains predominantly Cu^{+} and Zn^{2+}.

The crystallographic structure of rat liver MT-2 [8] is shown in Figure 1-2. This structure determination was made at a resolution of 230 pm and is currently being refined with a new data set at 190 pm [9]. The 7 metal ions are bound exclusively to the sulfur atoms of the 20 cysteine residues in two distinct metal-thiolate clusters. Residues 1-29 enfold the 3-metal 9-cysteine cluster, which is referred to as the ß domain. Residues 30-61 comprise the α domain, which enfolds the 4-metal 11-cysteine cluster. The unusual structure of MT has been described as a monolayer of

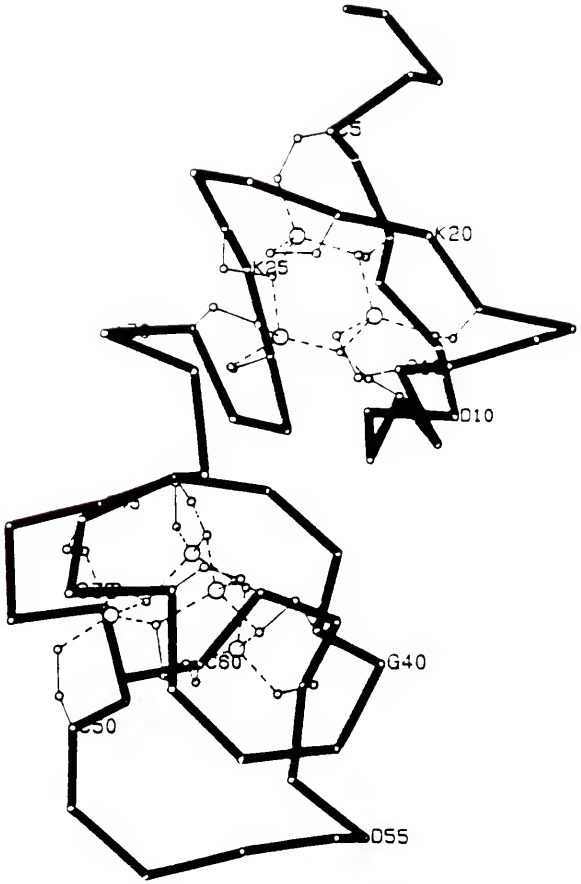

Figure 1-2. Crystallographic structure of rat liver MT-2. Shown are the α carbons of each residue, the ß carbons and sulfur atoms of each cysteine residue, and the Cd and Zn atoms. Reproduced from Furey et al. Science 1986, 231, 707 [8].

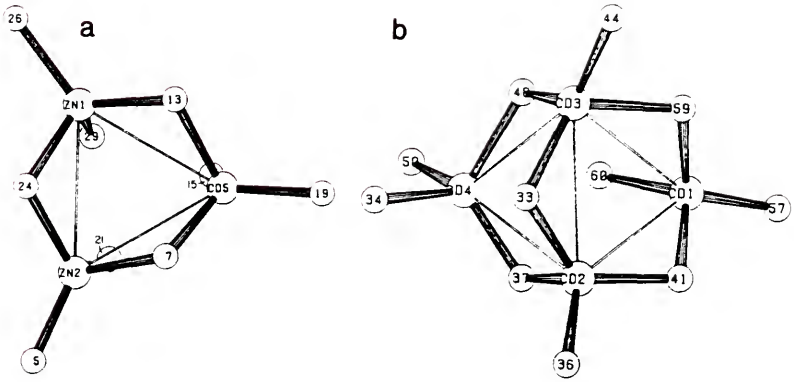

Figure 1-3. Expanded views of the structures of (a) the ß cluster domain and (b) the α cluster domain of rat liver MT-2. Shown are the cysteine sulfur atoms and the Cd and Zn atoms. Reproduced from Furey et al. Science 1986, 231, 707 [8].

polypeptide wrapping around the metal-thiolate clusters which take the place of the hydrophobic core of residues in a larger protein [8].

A detailed view of the crystallographic structures of the metal-thiolate clusters is shown in Figure 1-3. The ß cluster consists of 3 metal ions, 3 bridging thiolate ligands, and 6 terminal thiolate ligands. The metal ions and bridging thiolates form a 6-membered ring in a chair conformation. The adamantane-like structure of the α cluster is composed of 4 metal ions, 5 bridging thiolates, and 6 terminal thiolates.

The distribution of Cd^{2+} and Zn^{2+} ions among the 7 binding sites (as observed by ^{113}Cd NMR) is not a uniform one as shown in Figure 1-3. The relative numbers of Cd^{2+} and Zn^{2+} ions in a particular MT molecule and the distribution of these metals ions among the 7 binding sites vary from one molecule to the next. Apparent dissociation constants for Cd^{2+} and Zn^{2+} in MT ($K = [(cys)_3{}^{3-}][M^{2+}]/[(cys)_3M^{-}]$) have been estimated to be on the order of 10^{-15} M and 10^{-11} M respectively [10], based on spectrophotometric titrations of Cd_7MT and Zn_7MT with protons. Cd_7MT can be prepared via displacement of Zn^{2+} by adding excess Cd^{2+} salt to solutions of the native protein. Isolation of native MT in high yield is generally accomplished by administering a series of $CdCl_2$ injections to the animal so as to induce biosynthesis of MT prior to isolation. MT obtained in this

way contains both Cd^{2+} and Zn^{2+}. The Cd^{2+} is localized preferentially in the α domain and the more weakly bound Zn^{2+} in the ß domain.

Synthetic metal MT adducts have been prepared by three methods. Adducts may be prepared in vivo by injecting the animal with solutions of the metal ions of interest prior to isolation of the protein. The in vitro displacement of metal ions from native MT by added metal ions is another means of obtaining synthetic metal MT adducts. The third method entails reconstituting the apo (metal-free) form of MT with the desired metal ions in vitro.

MT adducts with Cu(I) [11], Hg(II) [12-14], Pb(II) [15], Au(I) [16], Bi(III) [17], Pt(II) [18], and other metals have all been prepared by the in vivo route. This procedure usually results in the recovery of mixed-metal MT adducts.

Metal MT adducts prepared by in vitro displacement of bound Cd^{2+} and Zn^{2+} from native and Zn_7MT include adducts with Cd(II) [19-23], Hg(II) [24, 25], Au(I) [26], and Pt(II) [18, 27]. Waalkes and coworkers have surveyed the ability of 16 different metals ions to displace Zn^{2+} from Zn_7MT [28]. Both mixed metal and single metal adducts have been prepared by this method.

Synthetic metal MT adducts prepared by reconstituting apoMT with various metals have been studied to the greatest extent. ApoMT is obtained by acidifying solutions of

native MT. At low pH the cysteine thiolates are protonated, and the metal ions liberated are removed from the protein solution by chromatography or exhaustive dialysis. Protocols for obtaining metallated derivatives of apoMT generally involve adding an excess of metal salt and then raising the pH to above neutral. The product or products are then desalted on a size-exclusion column. As the pH approaches the pK_a values of the cysteine sulfhydryls (ca. 8), the thiolates become unstable with respect to rapid air-oxidation to cystine disulfides. Reconstitutions are therefore performed under a nitrogen or inert gas atmosphere to prevent this undesirable denaturation. M_7MT adducts prepared from apoMT include adducts with Co(II) [29, 30], Ni(II) [29], Fe(II) [31], Cu(I) [32-34], Zn(II) [33, 35], Cd(II) [21, 23, 33, 35-39], Pb(II) [40], Hg(II) [40], and Bi(III) [40]. Neilson and coworkers have surveyed the binding of 18 different metal ions to apoMT [41].

Binding of Platinum(II) to Metallothionein

The potent anticancer agent cis-dichlorodiammine-platinum(II) (cisplatin) [42, 43] has been the subject of intense study since its antitumor activity was discovered [44] by Rosenberg et al. Most of this research has been concerned with the binding of cisplatin and analogous compounds to polynucleotides [45] as the mode of action of

these platinum drugs probably involves binding to DNA. The binding of platinum drugs to polypeptides and proteins has been studied to a far lesser extent [46, 47]. This aspect of the physiological action of cisplatin is important in understanding the toxicological effects of the drug. Cisplatin is known to cause extensive kidney damage as its primary toxicity, and this nephrotoxicity is one of the major dose-limiting factors in its therapeutic use [48]. In addition, the sequestering of Pt(II) from cisplatin by MT may be responsible for some of the reduction in the anticancer effect of the drug in repeated dose protocols.

Metallothionein is present in relatively high concentration in the cytosol of the kidney and is a probable binding site for platinum anticancer agents because of its abundance of cysteine residues and the N-terminal methionine. Platinum(II) is known to form very stable complexes with sulfur donor ligands [49]. The binding of Pt(II) to the sulfur bearing residues cysteine and methionine has been documented by protein crystallography wherein Pt(II) salts are used as heavy-atom labels [50].

The biodistribution of Pt in the tissues of experimental animals administered cisplatin intravenously has been described [51-53]. Platinum is rapidly cleared from the blood following injection, with filterable Pt in the plasma of rats declining to near zero after several hours [51, 53]. Tissue levels of Pt decline slowly over

about one week post-injection to leave several percent of the initial dose retained by tissue [51]. Cisplatin nephrotoxicity takes several days to manifest maximum severity during which the low molecular weight reaction products formed in the plasma are excreted into the urine and reabsorbed into the kidneys. By far the highest tissue concentration of Pt during metabolism of cisplatin is found in the kidney [51-53].

Sharma and Edwards found that at the time of maximum Pt accumulation in the rat kidney (ca. 24 hours post-injection) about 60% of cellular Pt in the kidney is localized in the cytosol [54]. This cytosolic Pt was partitioned into three main fractions by size-exclusion chromatography. Low molecular weight species (MW < 1000) accounted for 52% of the total Pt, 23% was found in the high molecular weight fraction (MW > 20000), and the remaining 25% eluted in a "metallothionein-like" fraction (6000 < MW > 12000) [54]. These observations and similar results reported by other workers [55, 56] suggest a possible role for MT in the detoxification of cisplatin and its metabolites.

Zelazowski and coworkers demonstrated that the total in vivo bound Pt in the kidneys of cisplatin treated rats can be significantly increased via induction of MT biosynthesis by preinjection with $CdCl_2$ [57]. MT-like size-exclusion fractions are composed of MT-1 and MT-2 as confirmed by gel electrophoresis. The authors also found

that binding of Pt from cisplatin in vivo and in vitro was associated with a large decrease in the Zn content (ca. 50%) of the native protein but only trivial Cd^{2+} losses. Binding of Pt(II) to native MT thus involves displacement of the relatively weakly bound Zn^{2+} ions.

Pt(II) may induce the biosynthesis of MT as has been documented for certain other heavy metal ions. However, several groups have presented evidence that stimulation of MT biosynthesis by Pt(II) is very minimal or nonexistent [57, 58].

Bakka et al. found that cultured cells with naturally high MT contents were resistant to the toxic effects of cisplatin [59]. This observation extends the hypothesis of heavy metal detoxification by MT and raises the interesting question of whether elevated MT concentrations might be used to alleviate the toxic effects of cisplatin and increase its effectiveness as an anticancer drug. However, tumor cells with higher MT concentrations might also be more resistant to the anticancer effects of cisplatin thus reducing the effectiveness of the drug. In another recent series of experiments, mutant tumor cells with elevated MT contents were implanted in mice and tumor growth following i.v. administration of cisplatin compared to a control group of mice implanted with wild-type cells [60]. Tumor volume was reduced by 80% in tumors from the parent cells, whereas the tumors from MT-rich cells were almost completely resistant.

Human carcinoma cells with high levels of MT, induced by chronic exposure to heavy metals and various anticancer drugs, are also known to acquire significant resistance to cisplatin [61].

Naganuma et al. have reported an increase in survival rates of mice injected with MT inducing metals prior to injection of a lethal dose of ciplatin [62, 63]. The greatest protection was imparted by preinjection with Cu(II) and Bi(III). This protective effect is presumably due to the binding of Pt(II) to MT but no direct relationship with the increased MT levels has been unequivocally established. A reduction in the lethal and renal toxicity of cisplatin without impairment of its antitumor activity in mice by preinjection with the MT inducer $Bi(NO_3)_3$ has been described recently [64].

The following chapters describe *in vitro* Pt(II) MT adducts from the reaction of K_2PtCl_4 with apoMT and the reactions of K_2PtCl_4 and cisplatin derivatives with Cd_7MT and native MT. This study is the first attempt to examine these adducts on the molecular level, and its primary aim is to provide synthetic models of the *in vivo* cisplatin MT metabolites reviewed above. The incorporation of square-planar Pt^{2+} ions in sites normally occupied by tetrahedral Cd^{2+} and Zn^{2+} ions is also of interest concerning the degree to which the structures of metal MT adducts are determined by the metal versus the polypeptide component of the adduct.

CHAPTER 2

PROTEIN DETERMINATION BY ICP-AES

The analytical method used to obtain bound metal stoichiometries and bound metal contents of metal MT adducts is described in some detail in this section as these are central results in the following study. The distinction between metal stoichiometries and metal contents is drawn here as some mixed metal MT adducts are heterogeneous with respect to the bound metal ions. In the native protein for example, Cd^{2+} ions preferentially occupy sites in the α domain while Zn^{2+} ions tend to reside mainly in the ß domain, but these two metal ions, as well as the lesser amounts of Cu^{+} and other bound metal ions, are not uniformly distributed across the binding sites of the protein. True binding stoichiometries can be obtained solely from analytical data only for single metal adducts for which stoichiometric binding occurs. For mixed metal adducts, on the other hand, true stoichiometries cannot be determined without some further information beyond the analytical data.

The analysis of metal MT adducts has traditionally involved the determination of the bound metal or metals by

one method and quantification of the polypeptide component by independent means. Metals can be conveniently assayed by either atomic absorption spectrometry (AAS) or inductively coupled plasma atomic emission spectrometry (ICP-AES). Determination of the polypeptide component, however, presents a more difficult analytical problem.

Protein concentrations are usually obtained on a routine basis by measuring the absorbance of micromolar solutions at the absorption maximum occurring at ca. 280 nm. This band arises from absorption by the aromatic side chains of tyrosine and tryptophan residues. The molar absorptivity must, of course, be arrived at by the use a molecular weight and some primary method of determining total protein. An accurate molecular weight is preferably obtained from amino acid sequence data, but a crude value obtained by hydrodynamic methods, such as size-exclusion chromatography or sedimentation, may have to suffice in some cases. The numerous existing methods of total protein determination include Nessler and Kjeldahl total nitrogen determinations, various direct colorimetric methods such as the Biuret, and the most simple and commonly used gravimetric or "dry weight" methods.

Unfortunately the ultraviolet spectrum of apoMT is devoid of a 280 nm peak due to its peculiar lack of aromatic residues. The spectrum contains an intense band at 190 nm arising from the strong π-π^* and weak n-π^* amide transitions

of the polypeptide backbone and the lowest thiol transition of the cysteine side chains near 195 nm [2]. The most commonly used method of estimating MT concentrations is to measure the absorbance of apoMT in 0.01 M HCl at 220 nm using a molar absorptivity of 48200 M^{-1} cm^{-1} [65]. This value was obtained by a wet chemical thiolate assay. The problems associated with the spectrophotometry of the sharply rising shoulder of this peak have been described thoroughly by Wetlaufer [66].

We have developed a method of obtaining micromolar protein concentrations and bound metal stoichiometries by ICP-AES of sulfur [67] which overcomes the shortcomings of traditional methods. Temperatures in an ICP torch are sufficiently high to excite many nonmetallic elements and several analytically useful emission lines in the vacuum ultraviolet have been observed [68]. Of particular interest to this study is the prominent sulfur line at 180.73 nm, which has an estimated detection limit of 15 µg/L [69]. Proteins with known contents of the sulfur bearing residues cysteine and methionine can thus be quantified at the µg level by ICP-AES, provided the instrument is equipped with evacuated or otherwise oxygen-free optics.

ICP-AES determinations of total sulfur in tissue samples [70, 71] and the use of an ICP-AES instrument as a sulfur detector in the HPLC of tissue extracts [72] have been reported. The purpose of the following experiments is

to demonstrate the viability of pumping micromolar purified protein solutions directly into the nebulizer of the ICP-AES instrument and determining protein concentrations based on the emission of sulfur at 180.73 nm.

Accuracy and Applications

Elemental analysis of proteins by ICP-AES has traditionally been restricted to metals in acid digested samples of metalloproteins. We initially sought to demonstrate that accurate absolute concentrations of proteins, regardless of the presence or absence of bound metals, can be obtained based on sulfur content by pumping buffered micromolar solutions directly into the nebulizer without any prior sample preparation, and using aqueous solutions of Na_2SO_4 as sulfur standards. The protein solutions, although relatively dilute, do have slightly different physical properties than the Na_2SO_4 standards, such as viscosity and surface tension, which could lead to differences in aerosol formation in the nebulizer and systematic errors in the results. One test of accuracy is to compare spectrophotometric molar absorptivities determined by ICP-AES of sulfur with published absorptivities based on traditional methods of protein determination (Table 2-1).

Table 2-1. Comparison of Spectrophotometric Molar Absorptivities of Proteins Based on ICP-AES of Sulfur with Published Values Based on Other Methods of Protein Determination.

Protein[a]	λ/nm	$\epsilon/10^4$ M^{-1} cm^{-1}			Ref
		ICP[b]	Lit[c]		
Cd_7metallothionein equine kidney MW 6.88 kD 21 mol S/mol					73
	250	10.9 ± 0.2	11.4	H	74
Ferricytochrome c equine kidney MW 12.4 kD 4 mol S/mol					75
	410	11.8 ± 0.3	11.20	B	76
			10.95	B	77
			10.60	B	78,79
	280	2.62 ± 0.06	2.40	D	80
			2.32	B	78,79
			2.12	D	81
Ferrimyoglobin equine MW 17.5 kD 2 mol S/mol					82
	409	17.9 ± 0.3	18.8	H	83
			18.6	C	84
			17.1	C	85
			16.0	H	86,79
	280	3.24 ± 0.05	3.2	H	87
			3.12	C	85

Table 2-1--continued.

Protein[a]	λ/nm	ε/10^4 M^{-1} cm^{-1}		
		ICP[b]	Lit[c]	Ref
Ribonuclease A bovine pancreas MW 13.7 kD 12 mol S/mol				88
	278	1.13 ± 0.02	1.19 A	89,79
			1.14 D,E	90,79
			1.13 H	91,79
			1.06 H	92,93
			1.04 D	94,93
			1.01 H	95
			0.98 H	96,79
Trypsin bovine pancreas MW 24.0 kD 14 mol S/mol				97
	280	3.72 ± 0.04	4.4 H	98,99
			4.14 D	100,79
			4.00 F	101,79
			3.98 D	102,79
			3.86 A	103,93
			3.86 H	104,93
			3.79 H	105,93
			3.74 D,F	81,93
			3.74 D	106,79
			3.72 H	107,79
			3.72 H	108,93
			3.69 G	109,93
			3.69 H	110,93
			3.67 A,D	111,93
			3.46 H	112,93

Table 2-1--continued.

Protein[a]	λ/nm	$\epsilon/10^4$ M^{-1} cm^{-1}		
		ICP[b]	Lit[c]	Ref
Chymotrypsinogen A bovine MW 25.6 kD 12 mol S/mol				113
	282	5.30 ± 0.11	5.30 F	114
			5.20 D	115,79
			5.20 D	116,79
			5.12 H	117
			5.12 H	118
			5.04 D	119
			4.13 D	120
	280	5.28 ± 0.11	5.32 D	80
			5.17 H	121
			5.15 H	122
			5.11 H	94,79
			4.61 F	123

[a] Molecular weights and sulfur contents were taken from amino acid sequences.

[b] (mean of sample - mean of blank) ± (standard deviation) for 6 replicate measurements of both sample and blank.

[c] Most of the ϵ values in this column were obtained from reported specific absorptivities ($A^{1\%}_{1cm}$) using the relationship: ϵ = MW $A^{1\%}_{1cm}/10$. Those values reported in the original literature as molar absorptivities (ϵ) are underlined. Also shown is the analytical method upon which the published value is based: amino acid analysis, A; colorimetric Fe determination, B; colorimetric heme determination, C; dry weight, D; Nessler N determination, E; Kjeldahl N determination, F; refractometry, G; no explicit reference to analytical method given, H.

While the list of published molar absorptivities in Table 2-1 is not an exhaustive one, it is an attempt to list as many literature values as possible in a nonselective manner [73-123]. The spread in the distribution of literature values for a particular protein is to be expected as each value was determined by different workers using the various analytical methods listed.

In general, very close agreement is found between the experimental molar absorptivities and the central tendencies of the published values. According to these comparisons the ICP-AES method of protein quantification via determination of sulfur is an accurate one, at least within the bounds of the concentration range and conditions described in the experimental section.

Probably the most useful application of the method is for the determination of metalloprotein binding stoichiometries. Bound metal stoichiometries are traditionally obtained by determination of the metallic component by atomic absorption or ICP-AES, and determination of the polypeptide component by independent means such as dry weight or total nitrogen determinations. These same stoichiometries, however, can be obtained by an ICP-AES determination of both components by using a single sample.

Shown in Table 2-2 are bound metal stoichiometries of three homogeneous proteins and metal contents of two heterogeneous metallothioneins as determined by ICP-AES of

Table 2-2. Metal Binding Stoichiometries and Metal Contents of Metalloproteins Determined by ICP-AES of Sulfur and Metals.

Protein	Metal	Mol Metal/Mol[a]
Native Metallothionein rat liver	Cd	3.02 ± 0.15
	Zn	3.18 ± 0.10
	Cu	0.26 ± 0.03
	total	6.46 ± 0.18
Native Metallothionein equine kidney	Cd	5.04 ± 0.36
	Zn	0.94 ± 0.08
	Cu	0.63 ± 0.23
	total	6.61 ± 0.41
Cd_7Metallothionein equine kidney	Cd	6.95 ± 0.040
Ferricytochrome c equine heart	Fe	0.955 ± 0.028
Ferrimyoglobin equine	Fe	0.900 ± 0.04[b]

[a] (mean of sample - mean of blank) ± (standard deviation) for 6 replicate measurements of both sample and blank.

[b] Spectrophotometric measurements indicated that this sample contained 90% holoprotein and 10% apoprotein.

sulfur and metals. Native metallothioneins have variable metal contents depending on the source and method of isolation. This variability is illustrated by the samples of MT from rat liver and equine kidney in Table 2-2. Concentrations of native MT cannot be satisfactorily determined by a metals assay because of this variability in metal contents. Concentrations can be accurately determined by a sulfur assay, however, as all mammalian metallothioneins have identical sulfur contents (21 mol S/mol MT). The sum of the Cd, Zn, and Cu contents for either native MT falls slightly below the maximum binding capacity of MT (seven divalent metal ions), but this probably results from the binding of minor amounts of Fe, Pb, Hg, and other metals not included in the assays.

The experimentally determined Fe content of ferrimyoglobin in Table 2-2 falls short of the true stoichiometry by about 10%. Spectrophotometric absorbance measurements of this sample taken at the Soret band at 409 nm arising from absorption by the iron containing heme moiety, and the band at 280 nm arising from aromatic side chains in the polypeptide portion of the molecule, also indicated the presence of 10% apoprotein, which lacks heme. The ferricytochrome c sample, that was purified extensively by ion-exchange chromatography, yielded an experimental result that is within 5% of the ideal stoichiometry.

Precision and Sensitivity

The standard deviations of the sulfur analyses in Table 2-1 are within 2% of the mean for 6 replicate measurements. The metal binding stoichiometries in Table 2-2 fall within 4-5% of the mean due to the uncertainties associated with both sulfur and metal determinations. This level of precision is acceptable for most applications particularly when one considers the rather poor reproducibility of many other existing methods of protein determination. If one wishes to make very fine distinctions (such as whether a certain protein binds 10 or only 9 metal ions) this level of precision becomes intolerable.

Small gains in precision might be realized by using optimized instrumental parameters for each element instead of compromise parameters, a pulseless syringe pump, improvement of power supply tolerance, and other refinements. The careful use of an internal standard [124] to mitigate precision-limiting flicker-noise in the nebulizer [125] may also improve precision.

The sensitivity of any destructive technique of protein determination is a general concern. We routinely obtain satisfactory results for samples with sulfur concentrations of 1 mg/L and higher. The volume of sample required is between 1 and 4 mL, which corresponds to the consumption of ten to several hundred micrograms of protein depending on

the molar sulfur content of the protein. While the sample volumes required for a pneumatic nebulizer are about two orders of magnitude greater than those required for a graphite furnace, they are not at all prohibitive in terms of the milligram scale on which protein research is often conducted.

Flow injection analysis (FIA) coupled with emerging total-consumption (direct injection) sample introduction systems could, in principle, reduce sample volumes from several milliliters to several microliters and greatly increase the applicability of ICP-AES to proteins [126]. FIA utilizes the transient signals generated by injecting small discrete sample "plugs" into a carrier stream and thus eliminates the wasteful dead-volume of the conventional continuous-flow mode of sample presentation. Experimental sample introduction systems with high transport efficiencies have been described and include a miniature concentric nebulizer installed in the injecter tube of a conventional ICP torch [127], and a thermospray vaporizer [128].

Advantages of the Method

The main advantages of protein determination by ICP-AES of sulfur, besides the high selectivity and multielement capability of atomic spectrometry in general, are the generality and rapidity of the method and the ease of sample

preparation. The method is applicable to any protein having a known content of sulfur. The only significant spectral interferences with the sulfur line at 180.73 nm are wing-overlaps of Ca and Mn lines which have intensities about two orders of magnitude smaller on a molar basis [129]. Perchloric acid digestion, dry ashing, and other time-consuming and error-prone preparatory steps are not necessary. A promising application of the method is the rapid and precise determination of metal binding stoichiometries in metalloproteins by determining both protein and metals for a single sample by a single method. In addition, ICP-AES is a useful method for determination of sulfur content of proteins following quantification of total protein by other methods.

Materials and Methods

Preparation of Samples and Standards

Horse kidney and rat liver metallothioneins were isolated and purified by a literature method [130]. Cd_7MT was prepared by adding excess $CdCl_2$ to a solution of native equine MT. An excess of the reducing agent dithioerythritol was added to ensure complete reduction of cysteine side-chains. After 24 hours the reaction mixture was fractionated on a Sephadex G-50 column. Horse heart cytochrome c was obtained from Sigma Chemical Company and

purified by carboxymethyl cellulose ion-exchange chromatography. The other proteins used in this investigation were obtained as lyophilized powders from Sigma and used without further purification. The ribonuclease sample was dissolved in 10 mM Tris/HCl buffer at pH 7.8. All other protein samples were dissolved in 5 mM phosphate buffer at pH 7.2. All samples were concentrated by ultrafiltration (YM5 membrane, Amicon Corp.) and then passed through a 0.2 μm filter (Gelman Sciences Inc.). The ultrafiltrates were used as blanks for both ICP-AES and spectrophotometric measurements. The metallothionein samples used for ICP-AES measurements had concentrations between 0.75-1.6 mg/L in sulfur. All other protein samples used were about 5 mg/L in sulfur.

Sulfur standards were solutions made from anhydrous Na_2SO_4. Standard solutions of the metallic elements were purchased from Aldrich Chemical Company.

Instrumentation

Elemental analyses were made by using a Perkin-Elmer Plasma II Emission Spectrometer equipped with a Perkin-Elmer Series 7000 computer. The one-meter Ebert monochromator (1800 l/mm holographically ruled grating) is sealed in a heavy-walled aluminum tube maintained at 5 mTorr. The path from the argon ICP source to the optical components was purged with a 5 L/min flow of nitrogen. The sample

introduction system is comprised of a peristaltic pump (12 rollers, silicone rubber pump tubing) and a cross-flow nebulizer [131]. Argon flow to the nebulizer is regulated by a mass flow controller. The following compromise operating parameters were employed:

RF Power	1200 W
Viewing Height	12 mm above coil
Sample Delivery Rate	1 mL/min
Argon Flow Rates	
plasma	15 L/min
auxiliary	1 L/min
nebulizer	1 L/min

Absorbance measurements were recorded on an IBM 9430 UV-Visible spectrophotometer. Samples were diluted to give absorbance values between 0.5 and 1.0 in a 1 cm path-length quartz cell.

Measurements

Individual ICP-AES measurements were obtained by scanning a 0.020 nm window centered on the emission line of interest and recording intensity counts at the wavelength of maximum emission. For multielement analyses the monochromator slews from one emission line to the next in a sequential fashion. The emission lines scanned were

S I 180.73, Fe II 259.94, Cd II 214.44, Zn I 213.86, and Cu I 324.75 nm. Six replicate measurements were recorded for each element of each standard, sample, and blank. Linear calibrations were obtained immediately prior to running each protein sample and corresponding ultrafiltrate blank.

CHAPTER 3
PLATINUM(II) BINDING TO APOMETALLOTHIONEIN

The first goal of the research was to investigate Pt(II) MT adducts prepared from mixtures of apoMT and K_2PtCl_4. This chapter describes the preparation and spectroscopic characterization of such adducts. The dynamics of the binding process are also examined in some detail. Spectra and other experimental results obtained for the synthetic Pt(II) adducts are compared, wherever practical, with corresponding data obtained for the widely studied native form of the protein.

Basic Physical and Chemical Properties of Platinum(II) Adducts of Apometallothionein

A change from a colorless to a yellow solution occurs when micromolar solutions of apoMT at neutral pH are mixed with excess K_2PtCl_4. The resulting adduct contains 6.95 ± 0.24 mol Pt/mol MT as determined by ICP-AES determinations of platinum and sulfur. The ICP-AES method was used, unless stated otherwise, for all the elemental analyses reported in this work, and is described in detail in Chapter 2. Dozens of reconstitutions have been performed and the

resulting products invariably contain 7 mol Pt/mol MT. Once formed, Pt_7MT is air-stable, and solutions have been stored for up to 6 months at 6°C without loss of bound Pt^{2+} or chromatographic evidence of aggregation.

Pt_7MT elutes as a single symmetrical peak on a Sephadex G-75 size-exclusion column (Figure 3-1a). Dimeric, trimeric, and higher oligomeric species are also isolated when the reactants are mixed at higher concentrations. These oligomers are also found to contain approximately 7 mol Pt/mol MT. A similar elution profile is often observed for solutions of native MT, and the oligomerization is probably due to a small number of intermolecular disulfide linkages formed by partial oxidation of the cysteines during isolation or storage [19]. Oxidation of the cysteines can be reversed by 2-mercaptoethanol and other reducing agents. Sephadex G-75 is the chromatographic gel of choice for MT, but even G-50 resin provides sufficient resolution to separate monomers from oligomeric species (Figure 3-1b).

The Stokes' radius of native MT, as determined by size-exclusion chromatography, is equivalent to that of a much higher molecular weight globular protein. Stokes' radius is defined as the radius of an equivalent hydrodynamic sphere. The large Stokes' radius of MT is due to the nonglobular elongated shape of the molecule (Figure 1-2). Pt_7MT has a slightly larger Stokes' radius (ca. 1.80 nm) than Cd_7MT or native MT (both ca. 1.60 nm). These radii were determined

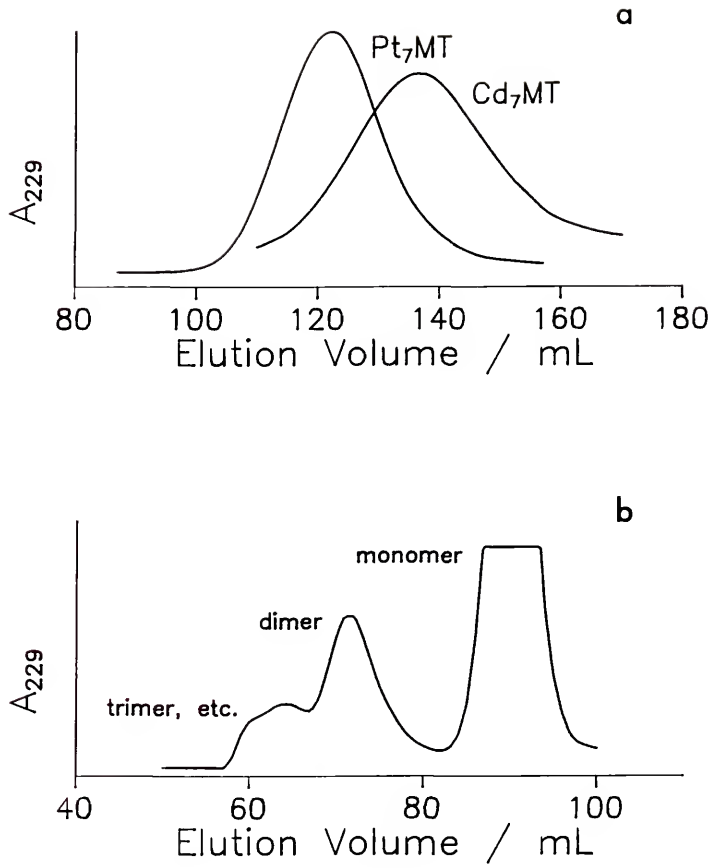

Figure 3-1. Elution profiles of (a) Cd_7MT and Pt_7MT on a Sephadex G-75 size-exclusion column and (b) native MT on a G-50 column. The eluant was 3.5 mM phosphate buffer, pH 7.2, and the column was monitored by the absorbance at 229 nm (A_{229}).

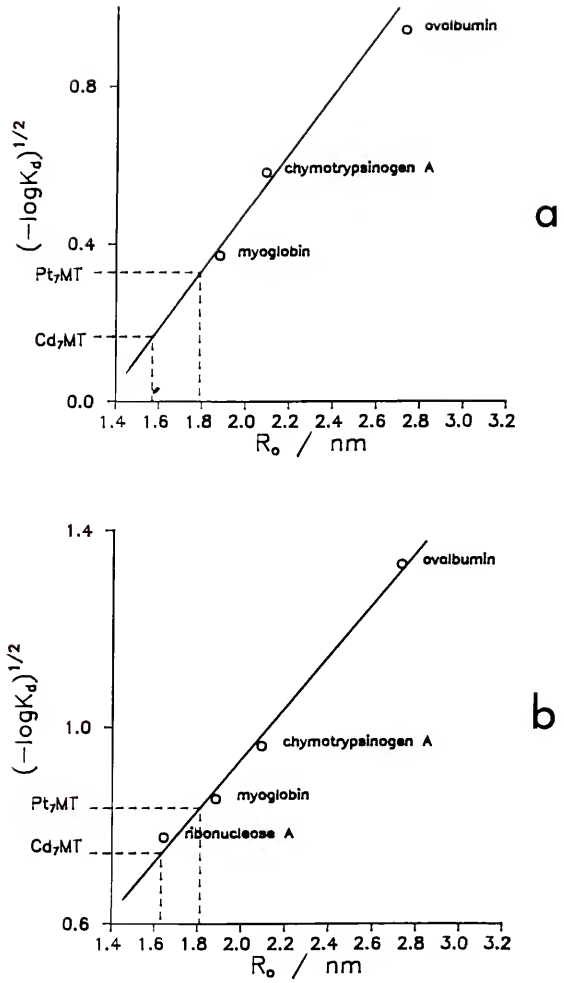

Figure 3-2. Stokes' radii of Pt_7MT and Cd_7MT determined by using calibrated Sephadex (a) G-75 and (b) G-50 size-exclusion columns.

were determined by using Sephadex G-50 and G-75 columns calibrated against globular proteins with known Stokes' radii (Figure 3-2) [132].

The Stokes' radius of Pt_7MT is consistent with retention of the two domain structure of the native protein and Cd_7MT. This is necessary but not sufficient evidence that Pt_7MT has the two domain structure, or any fixed conformation, as we have estimated the Stoke's radius of a hypothetical random coil polypeptide of 61 residues to be very close to radii obtained for Pt_7MT and Cd_7MT [27].

We are not certain if Pt_7MT is homogenous with respect to charge. Ion-exchange chromatography on DEAE cellulose against a 0.15 M KCl gradient gave a single extremely broad elution band. Nondenaturing polyacrylamide gel electrophoresis gave a similar result. The adduct recovered from the ion-exchange procedure contained 5.67 ± 0.34 mol Pt/mol MT. The tenacious binding of Pt_7MT to the ion-exchange and electrophoresis media, and the loss of roughly one mol equiv of Pt^{2+}, might be the result of a slow binding of Pt^{2+} ions to the pendant amino groups on the media. It is possible that one of the bound Pt^{2+} ions in Pt_7MT is relatively exposed to solvent, possibly a Pt^{2+} ion bound to the N-terminal methionine. Binding of Pt(II) to the exposed methionine residues of proteins is well known [47] and Pt(II) salts have been used extensively as heavy atom labels by protein crystallographers [50].

Further experimental evidence supporting a bound Pt^{2+} at the methionine (met-1) was obtained by examining the extent to which Cd^{2+} and Pt^{2+} bind to apoMT chemically modified at the methionine residue. The N-terminal methionine of apoMT was converted to methionine sulfoxide, a much poorer ligand for Pt(II), by an oxygen atom exchange reaction with excess dimethylsulfoxide [133] to yield the modified MT and dimethylsulfide as the other product. Reconstitution with $CdCl_2$ and K_2PtCl_4 followed by ICP analysis of the adducts showed that while the modified apoMT still bound the full complement of 7 Cd^{2+} ions (7.10 ± 0.29 mol Cd/mol MT), the binding of Pt^{2+} was indeed decreased by approximately one mol equiv (5.79 ± 0.60 mol Pt/mol MT). This evidence alone is not sufficient to prove that Pt^{2+} binds to met-1, but it is highly unlikely that this would not occur based on the known chemistry of Pt(II) and this amino acid.

The bound metal ions in Pt_7MT are not liberated from the protein under acidic conditions (as occurs for Cd_7MT and other adducts). Dialysis of Pt_7MT against 1 M HCl did not result in the loss of bound Pt^{2+} and no further binding occurs at this pH following the addition of excess K_2PtCl_4. The average binding constant for Pt_7MT must be many orders of magnitude higher than that of Cd_7MT which remains fully metallated only at pH ≥ 5 [134].

The great stability of the Pt^{2+}-to-cysteine-thiolate complexes is further evidenced by the observation that apoMT reacts with excess K_2PtCl_4 at pH 2 to form polymeric adducts containing 17 ± 1 mol Pt/mol MT. The degree of binding indicates that an essentially one-to-one Pt-to-cysteine coordination is occurring. The binding of slightly less than 20 Pt^{2+} ions and the polymeric nature of the products can both be attributed to intermolecular S-Pt-S bridging. As the amino acid sequence of MT contains three pairs of adjacent cysteines (Figure 1-1) it is also possible that a small proportion of the Pt^{2+} ions are coordinated in a bidentate fashion to two adjacent cysteines. The apparently random mode of binding at low pH may be a result of the much slower rate of binding or the reported random coil structure of apoMT at low pH [135].

Pt_7MT is also quite stable to displacement of Pt^{2+} ions by other electrophiles, such as the oxidizing agent 5,5'-dithiobis(2-nitrobenzoic acid) (DTNB) and the alkylating agent iodoacetate (Figure 3-3). At neutral pH, Pt_7MT reacts with the cysteine assay reagent DTNB at an initial rate ca. 8 times slower than found for the reaction of the apo protein under the same conditions [37]. Iodoacetate reacts with Pt_7MT ca. 15 times slower than reported for the reaction of iodoacetamide with apoMT under the same conditions. These rate reductions are nearly twice those found for the reactions of Cd_7MT with DTNB and iodoacetamide

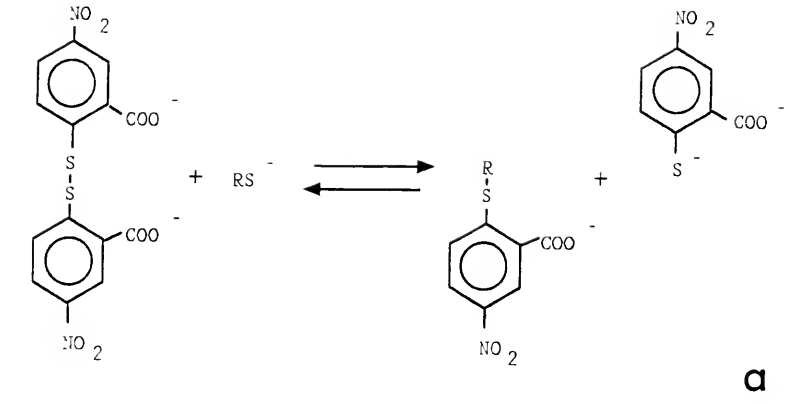

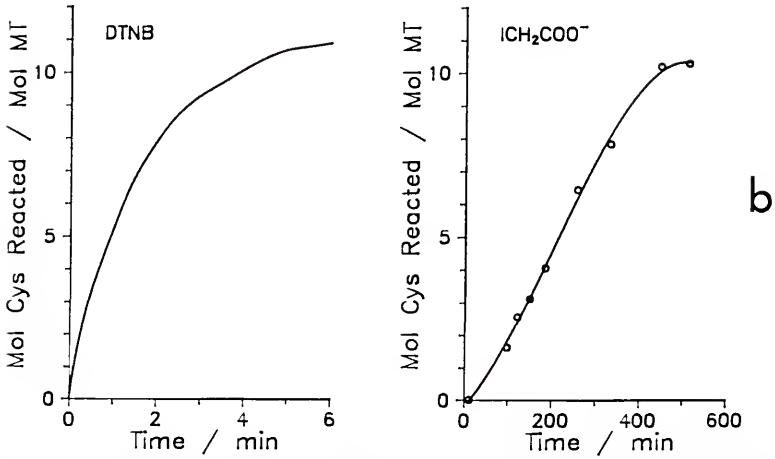

Figure 3-3. Shown are (a) reactions of DTNB and iodoacetate with thiolates and (b) time courses for the reactions of 1.0 mM DTNB with 1.7 μM Pt_7MT and 1.0 mM iodoacetate with 9.0 μM Pt_7MT at neutral pH.

[37], which is consistent with the known decrease in reactivity of the cysteine thiolates with stronger metal-to-sulfur bonds. Roughly half of the 20 cysteines in Pt_7MT reacted with either reagent. ICP analysis of the products showed that no Pt^{2+} ions were displaced from the protein in either of the two reactions.

All seven Pt^{2+} ions are liberated from Pt_7MT, however, by dialysis against excess cyanide to form highly stable $Pt(CN)_4^{2-}$. Complete removal of Pt^{2+} from 35 μM Pt_7MT by equilibrium dialysis in 0.1 M NaCN at pH 7.0 was confirmed by both spectrophotometric and ICP-AES measurements of the products. ApoMT was recovered from this dialysis in its completely reduced form, i.e. no characteristic cystine disulfide peak at 280 nm was observed in the ultraviolet spectrum. Air-oxidation of cysteine pairs to cystine disulfide groups is presumably followed by redox reaction with CN^- yielding cys^- and cys-SCN [136]. Dialysis of Pt_7MT against CN^- or other ligands with high affinity for Pt(II) under acidic conditions could be used to recover intact apoMT from Pt_7MT.

Optical Spectra

The electronic absorption spectrum of Pt_7MT consists of a broad region of absorption similar to the spectra of other metal MT adducts (Figure 3-4). The spectrum is consistent

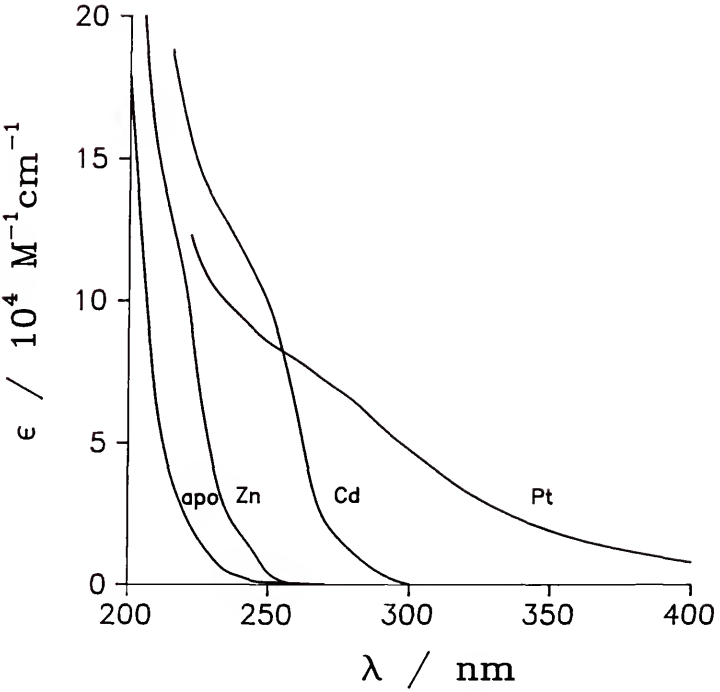

Figure 3-4. Electronic absorption spectra of apoMT, Zn_7MT, Cd_7MT, and Pt_7MT.

with the presence of Pt^{2+} to cysteine thiolate coordination as well as possible coordination of Pt^{2+} to the thioether sulfur of met-1. As illustrated in Figure 3-4, Pt_7MT follows the general trend of the absorption spectra of MT adducts with heavier metals to extend to longer wavelengths [2]. The spectra of Cd_7MT and Zn_7MT are similar in shape and intensity to those of Cd(II) and Zn(II) complexes of 2-mercaptoethanol which are arise from thiolate-to-metal charge-transfer transitions [134]. The spectrum of Pt_7MT also contains weak d-d ligand field bands in addition to intense thiolate-to-Pt charge-transfer components.

The electronic absorption spectrum of Pt_7MT is similar to the spectra of other metal MT adducts in that it is complex and difficult to interpret. Some interesting information about Cd_7MT, however, has been obtained from a spectrophotometric titration of apoMT with Cd^{2+} ions [38]. We have performed a similar experiment to study the binding of Pt^{2+} ions to apoMT.

Figure 3-5 shows the spectra of partially platinated Pt(II) apoMT adducts recorded for a series of apoMT solutions equilibrated with 1-8 mol equiv of K_2PtCl_4 at pH 7.5. Also shown are the incremental difference spectra obtained by subtracting from each spectrum the spectrum preceding it. The simple approach of adding increments of K_2PtCl_4 to a single solution of apoMT was not practical here as Pt(II) binding to apoMT at these low concentrations is

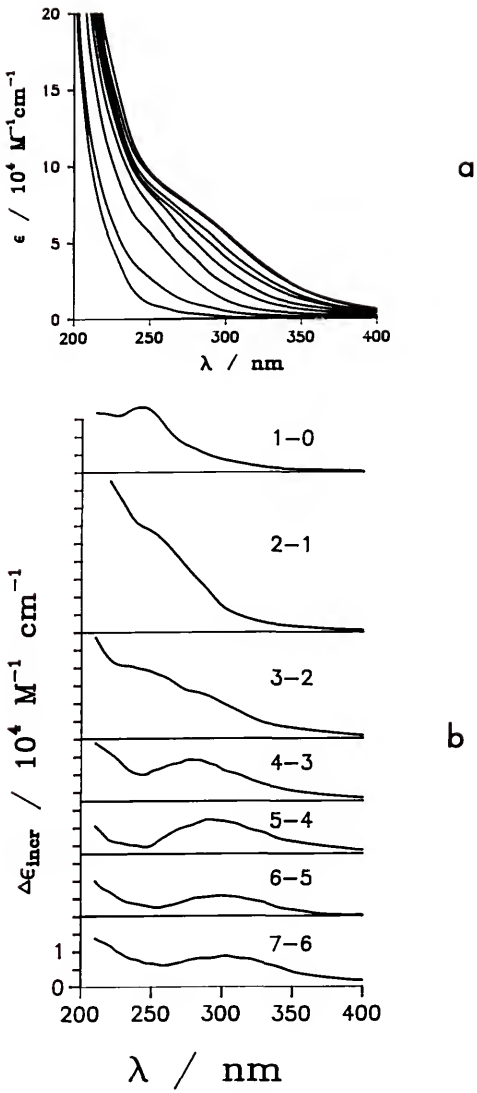

Figure 3-5. Spectrophotometric titration of apoMT with K_2PtCl_4 at pH 7. Shown are (a) the spectra resulting from the addition of 0 to 8 mol equiv of K_2PtCl_4 to apoMT and (b) the incremental difference spectra obtained by the subtracting the preceding spectrum from each spectrum.

very slow requiring about an hour to ensure equilibrium for each step. These long reaction times would be troublesome in the latter type of experiment as solutions of the apoMT at neutral pH are exceedingly sensitive to rapid air-oxidation.

Binding of the first mol equiv of Pt^{2+} to apoMT results in an absorption peak centered at about 250 nm. A very intense shoulder of absorption appears at ca. 250 nm after binding of the second mol equiv of Pt^{2+}. The incremental difference spectrum for the third mol equiv of Pt^{2+} contains two broad maxima at 250 and 300 nm. Mol equiv 4-7 result in absorption peaks of diminishing intensity at ca 280-300 nm. These data confirm the earlier finding that apoMT becomes saturated after binding 7 mol equiv of Pt^{2+}.

Wilner and coworkers observed a 6 nm red shift in the incremental difference spectra when apoMT was titrated with more than three mol equiv of Cd(II) [38]. A decrease in the intensity of the absorption in the later stages of the titration (>3 mol equiv Cd^{2+}) was also observed. Good and Vasak also report a red shift in the electronic absorption spectra recorded during step-wise incorporation of Fe(II) into apoMT [31]. These red-shifts as the titration of apoMT exceeds three mol equiv of metal ions have been attributed to the onset of thiolato bridging.

The first three metal ions presumably bind to three separate sets of terminal thiolate ligands to form three

$M(cys)_4^{2-}$ units. Binding of the remaining four metal ions involves the formation of bridging thiolates from the remaining uncoordinated thiolates as well as transformation of some terminal thiolates to bridging thiolates [38]. Supporting evidence for this inferred mechanism was provided by spectra of Cd(II) complexes with the synthetic tetrathiol dodecapeptide, P-12 (Ac-P-C-Ornithine-C-P-Q-C-Q-C-R-R-V) [38]. Titration of P-12 with Cd(II) yields sharp breaking points at 1:1 and 2:3 molar peptide-to-Cd ratios presumably due to the formation of a monomeric mononuclear complex and a dimeric trinuclear complex, respectively. The band maximum of the monomeric complex red-shifts ca. 6 nm as excess Cd^{2+} is added and bridging thiolates are created upon formation of the trimeric complex [38].

Further evidence for this mechanism of cluster formation comes from an EPR study of Co(II) binding to apoMT done by Vasak and Kagi [137]. A linear increase in the room temperature EPR signal intensity occurs with titration of apoMT with 3-4 mol equiv of Co(II) ions followed by a linear decrease in intensity to zero with the addition of further ions to the saturation point of 7 mol equivalents. The EPR spectrum of Co_7MT is characteristic of high spin tetrahedral Co(II) and is observed only at liquid helium temperatures. The loss of paramagnetism at higher temperatures is due to antiferromagnetic coupling between thiolato bridged Co(II) ions. The EPR titration data also

suggest that the first 3-4 Co(II) ions bind to separate sets of terminal thiolates and that bridging and cluster formation occur after this initial process.

We have obtained evidence that the above mechanism is operative in the binding of Pt(II) to apoMT by use of the colorimetric thiolate assay reagent, DTNB. As discussed in the previous section, DTNB reacts many times slower with thiolates coordinated to Pt^{2+} than with free thiolates. This difference in reactivity makes it possible to determine the concentrations of both coordinated and free thiolates at each step in the titration of apoMT with Pt^{2+}. This experiment is not amenable to the study of Cd^{2+} and Zn^{2+} binding to apoMT as bound Cd^{2+} and Zn^{2+} do not sufficiently slow down the reaction of DTNB with thiolate.

Figure 3-6 shows the results obtained when each of the solutions used in the spectrophotometric titration were allowed to react for one minute with a 315:1 molar excess of DTNB:MT under anaerobic conditions. It is clear that the first 3 mol equiv of Pt^{2+} coordinate to 4 cysteine thiolates per Pt^{2+}. Binding of the remaining 4 mol equiv of Pt^{2+} ions occurs by coordination to progressively fewer thiolate ligands per Pt^{2+} ion. Roughly two thiolates are found to react with DTNB during the time permitted after the apo protein is saturated with the full complement of seven Pt^{2+} ions. This residual reactivity is due either to two uncoordinated thiolates in Pt_7MT or two relatively reactive

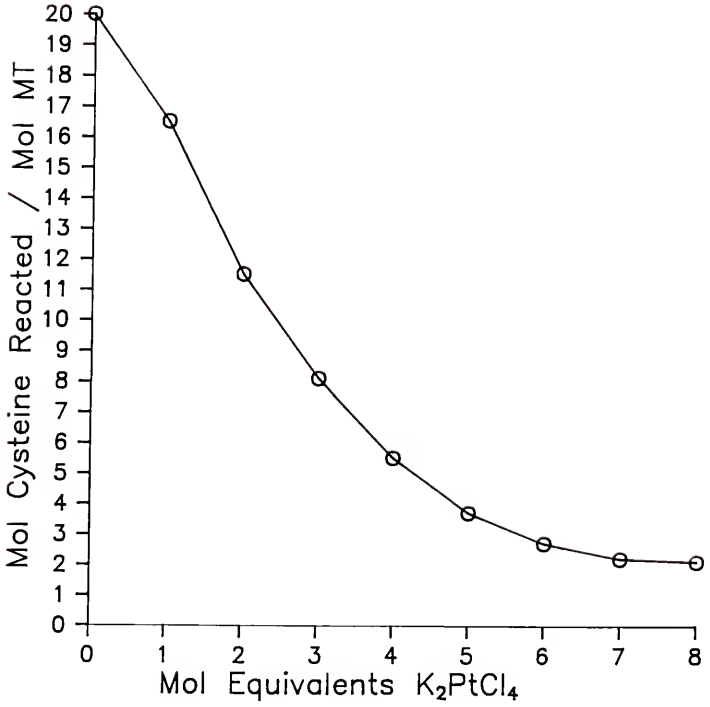

Figure 3-6. Titration of the partially platinated apoMT adducts from each step of the spectrophotometric titration with the thiolate assay reagent, DTNB.

coordinated thiolates being present. The reactivity of DTNB with Pt^{2+} bound thiolates will vary depending on many factors, primarily the bond strength of the individual group and the accessibility to the reagent solution. It is possible, for instance, that two bridging thiolates in Pt_7MT are relatively exposed to the surrounding medium.

The changes in the maxima of the ultraviolet spectra that occur upon the addition of more than 3 mol equiv of Pt^{2+} to apoMT can be accounted for by the formation of bridging thiolates and the transformation of terminal thiolates to bridging thiolates. In attempting to explain the apparent red-shift of the ligand-to-metal charge-transfer (LMCT) absorption maximum that coincides with this change in the mode of Pt^{2+} binding, it is helpful to compare the electronic spectra of Pt(II) tetrahalides (PtX_4^{2-}) with the spectra of their dihalo bridged dimers ($Pt_2X_6^{2-}$).

Figure 3-7 is a molecular orbital diagram for a PtX_4^{2-} complex showing the three allowed LMCT transitions. The LMCT spectra of the square-planar tetrahalide complexes of Pt(II), Pd(II), and Au(III) consist of two intense bands separated by about 9000-12000 cm^{-1} [138]. The first, lowest energy, absorption band ($\epsilon \approx 1 \times 10^4$ M^{-1} cm^{-1}) originates from the two closely spaced $M\sigma^* \leftarrow L\pi$ transitions and the second, more intense, band ($\epsilon \approx 4 \times 10^4$ M^{-1} cm^{-1}) originates from the $M\sigma^* \leftarrow L\sigma$ transition. For the tetrachloro and tetrabromo complexes, the energy of the first allowed band

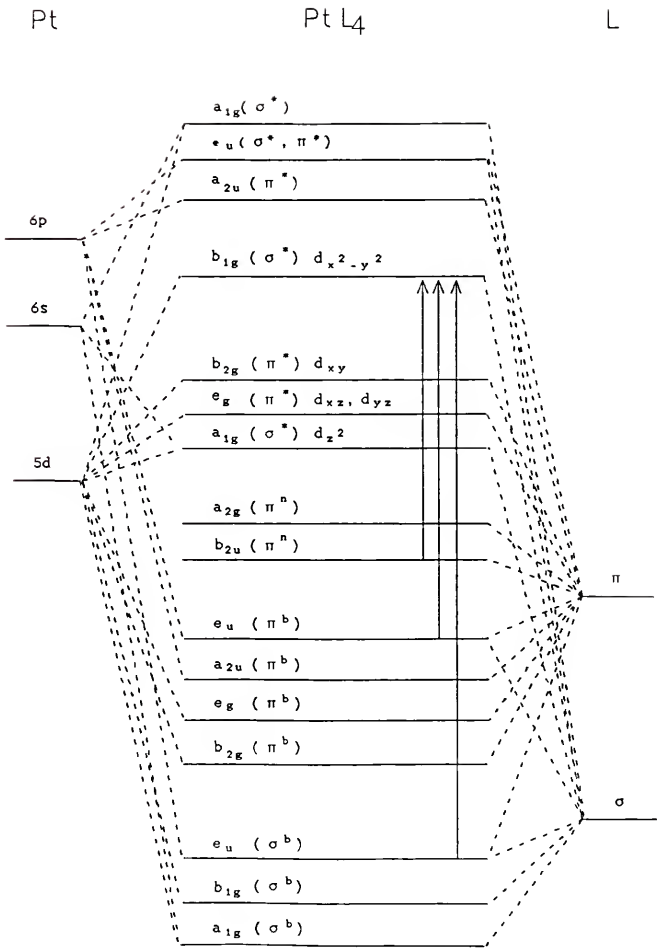

Figure 3-7. Relative molecular orbital energies estimated for square-planar Pt(II) complexes.

increases in the order: $AuBr_4^-$ < $PdBr_4^{2-}$ < $AuCl_4^-$ < $PdCl_4^{2-}$ < $PtBr_4^{2-}$ < $PtCl_4^{2-}$. For PtX_4^{2-}, the $M\sigma^* \leftarrow L\sigma$ band usually occurs at wavelengths too low to be experimentally observed.

The dihalo bridged dimers of Pt(II) and Pd(II) typically have intense absorption bands which lie 30-60 nm below the first LMCT bands of the corresponding monomers [139-142]. This behavior was observed for $(Bu_4N)_2Pd_2Cl_6$ and $(Bu_4N)_2Pd_2Br_6$ in glasses at 77 K in an early study by Mason and Gray [141] who speculated that these bands arose from the transfer of nonbonding π electrons from the bridging ligands to Pt.

However, more recent polarized crystal spectra of $(Et_4N)_2Pt_2Br_6$ [139] show that this first LMCT band must arise from transfer of π electrons from the terminal ligands. In order to understand this observation it is necessary to consider separately the two sets of molecular orbitals formed by the bridging and terminal ligands in the D_{2h} dimer. Defining the x-axis as normal to the plane of the molecule, one finds that while the p_x orbitals of the bridging (p_{xb}) and terminal (p_{xt}) bromines both form pure out-of-plane π MO's, the p_{yb} and p_{zb} orbitals are involved in σ bonding only, and cannot be combined into σ and in-plane π MO's as obtained for p_{yt} and p_{zt}. Since the first intense band in the crystal spectrum of $(Et_4N)_2Pt_2Br_6$ (317 nm, 9000 M^{-1} cm^{-1}) is the only strong band in z

polarization up to 270 nm, it must assigned to $M\sigma^* \leftarrow L\pi$ transitions originating from the terminal bromines [139].

The occurrence of the first $M\sigma^* \leftarrow L\pi$ LMCT band of $(Et_4N)_2Pt_2Br_6$ at a wavelength 49 nm longer than that of K_2PtBr_4 [143] can be explained by using a very simple argument [139]. The Pt atoms in the dimer should be more electronegative than the Pt atom in the monomer because there are fewer bromides per Pt in the dimer to donate electronic charge. It is not surprising, then, that the first LMCT transition in the dimer should occur at lower energy than in the monomer as it is well known, from the work of Jorgensen [144], that the energy of this band can be correlated with the difference in electronegativities of metal and ligand. Delocalization within the central $Pt(\mu\text{-}X)_2Pt$ region may also stabilize LMCT excited states of the dimers. The red-shifting and decrease in intensity of the band maxima of the incremental difference spectra in the later stages of the spectrophotometric titration of apoMT with K_2PtCl_4 (Figure 3-5a) are completely consistent with a decrease in the number of terminal thiolates versus bridging thiolates and a lowering in energy of the $M\sigma^* \leftarrow L\pi$ LMCT transitions for these terminal thiolates due to presence of bridging thiolates.

It is also possible that some shifting of the LMCT bands to longer wavelengths results from a distortion of the ligand geometry at the Pt centers from D_{4h} to D_{2d}

symmetry. The lowest lying LMCT band of the tetrahedrally distorted Pt(II) complex with the sterically hindered PEt_3 ligand (P-Pt-P angles are ca. 150^{o}), to take an extreme example, is found to be red shifted about 30 nm from the corresponding band for the planar bis(1,2-diethylphosphino)ethane complex [145]. However, it is not necessary to invoke this effect, and large distortions from square-planar geometry in these Pt(II) MT adducts do not appear to be energetically feasible because of the very large ligand field stabilization energies that would have to be overcome. Distortion of $PtBr_4^{2-}$ (Δ_1 = 2.75 eV, Δ_2 = 0.74 eV, Δ_3 = 0.44 eV) to the tetrahedral limit ($\Delta \approx 1.22$ eV = $4\Delta_1/9$), for example, would theoretically require 2.71 eV [138]. By comparison, the Gibbs' energy of a typical intramolecular hydrogen bond in a protein is only about 0.20 eV in aqueous solution [146]. The strongest hydrogen bonding is found in the hydrophobic interiors of proteins [146], and the interior of MT is unusual in that it contains metal-thiolate clusters rather than a hydrophobic core of amino acid residues. It seems reasonable, then, to expect that the structure of a metal MT adduct is largely dictated by the energetics of metal-thiolate cluster formation. However, the net forces of intermolecular hydrogen bonding exerted by the surrounding polypeptide chain of metal MT adducts are likely to cause slight distortions, even in the case of Pt(II).

The circular dichroism spectra of apoMT containing 0 to 7 mol equiv of bound Pt^{2+} (Figure 3-8) are more difficult to interpret than the corresponding electronic absorption spectra. Ellipticity bands in the spectra of metal MT adducts contain contributions from both the conformationally dependent configurational chirality of the polypeptide and charge-transfer from the chiral cysteine thiolate ligands to the metal ions. Optical activity above 240 nm, however, contains only contributions from the asymmetric charge-transfer components [147].

The CD spectrum of apoMT at neutral pH is similar to its electronic absorption spectrum in that it is nearly devoid of spectral information except for a sharply decreasing negative ellipticity band beginning at about 240 nm and extending into the far ultraviolet. As shown in Figure 3-8, the addition of the first mol equiv of Pt^{2+} brings about a single positive ellipticity band centered at about 250 nm. Addition of mol equiv 2-3 result in a significant drop in the (+) intensity of the spectrum but very little change in its shape. The (+) intensity of the 250 nm maximum rises abruptly after the addition of 4 mol equiv of Pt^{2+} and remains fairly unchanged through 6 mol equiv, although there is some broadening of the spectrum in the region 250-300 nm. Binding of the seventh and final mol equiv of Pt^{2+} causes a large increase in the (+) intensity

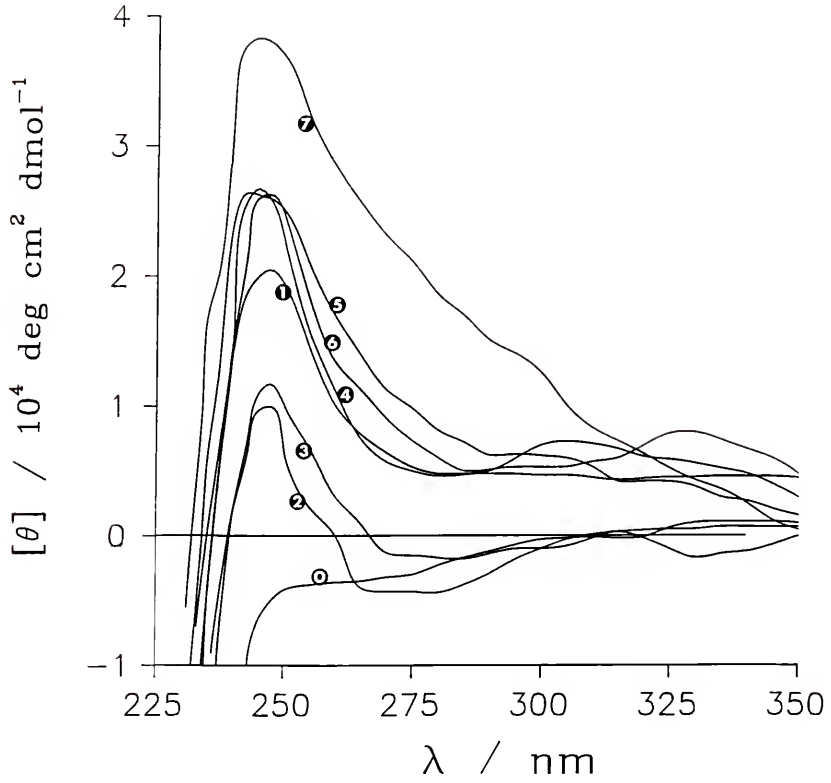

Figure 3-8. Titration of apoMT with 0 to 7 mol equiv of K_2PtCl_4 as followed by circular dichroism.

of the spectrum giving a broad shoulder of ellipticity similar to that of the electronic absorption spectrum.

Abrupt changes in CD spectra upon addition of the fourth mol equiv of metal ions have also been observed for partially metallated adducts of apoMT with Cd^{2+} and Zn^{2+} ions [21]. One interpretation of the spectral changes observed for Pt(II) binding is that major changes in the conformation of the protein occur during binding of the first 3 mol equiv of Pt^{2+} ions, which entails the coordination of 4 cysteine ligands for each Pt^{2+} ion as shown by the DTNB assays. The fact that the CD features undergo practically no change at all for adducts containing 4-6 mol equiv of Pt^{2+} is attributable to the inclusion of these additional bound ions into preformed metal-thiolate clusters via the formation of bridging thiolates. This interpretation relies heavily upon the common assumption that the CD spectra of metal MT adducts in general are ligand based, i.e. changes in rotary strength are linked to configurational changes in the cysteine ligands which occur with metal binding [2]. A similar lack of CD spectral changes following the addition of 4 mol equiv of metal ions has been found for the titration of apoMT with Cd^{2+} ions [21].

The large (+) increase in the CD intensity observed for the binding of the seventh and final mol equiv of Pt^{2+} is somewhat peculiar. We have suggested that one of the Pt^{2+}

ions in Pt_7MT is bound to the N-terminal methionine residue, and it is reasonable to expect that this neutral ligand is thermodynamically and kinetically less reactive than the cysteine thiolates [49]. It is expected, then, that binding to methionine will occur only after saturation of the cysteine thiolate ligands. The binding of the seventh Pt^{2+} ion to met-1 would produce a new chiral center at the thioether sulfur, and possibly a conformational alteration of the first several residues in this portion of the molecule, giving rise to a significant change in the CD spectrum.

The far-UV CD spectra of apoMT (Figure 3-9) and native MT (Figure 3-10) both contain a strong negative ellipticity band near 200 nm. This band is similar to that observed for random coil polypeptides and is a reflection of the lack of secondary structure in both the apo and metallated forms of MT as confirmed by the crystallographic structure (Figure 1-2). The native protein contains essentially no α-helix or ß-sheet regions. The crystallographic structure does show a considerable number of ß-turns which were also indicated by an earlier Raman and infrared absorption study which found MT to be a "predominantly turn-containing protein" [148]. The lower intensity of the 200 nm ellipticity band for native MT as compared with apoMT probably results from an increase in the number of ß-turns in the folded metallated form of MT. A decrease in the

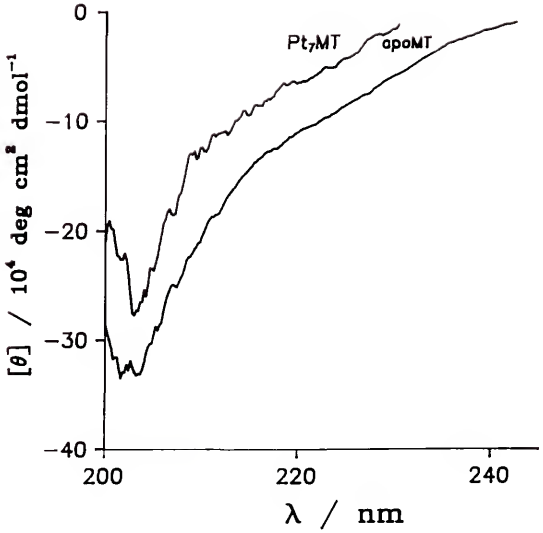

Figure 3-9. Circular dichroism spectra of apoMT and Pt_7MT in the far ultraviolet.

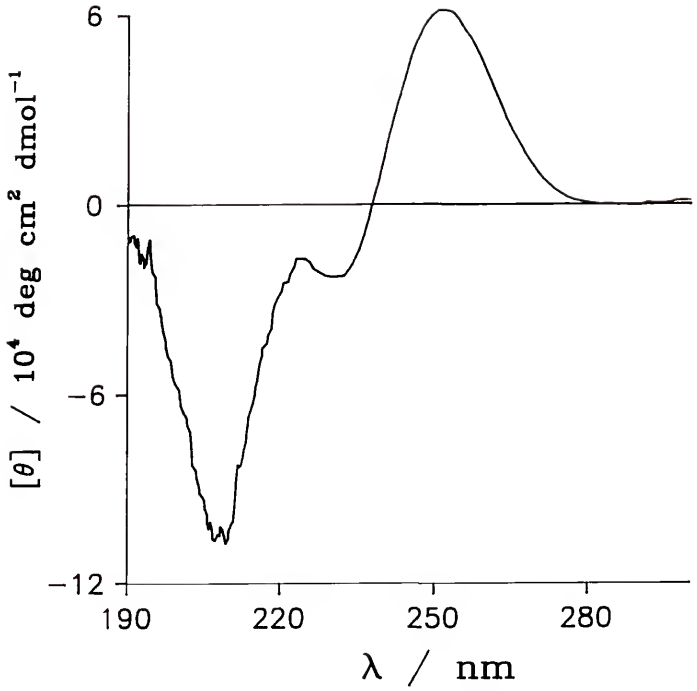

Figure 3-10. Circular dichroism spectra of native rat liver MT in 3 mM phosphate buffer pH 7.2.

intensity of this band for Pt_7MT compared to apoMT probably also results from a similar structural organization during Pt^{2+} binding.

Nuclear Magnetic Resonance Spectra

NMR spectroscopy has become increasingly important in the study of the structure and dynamics of metallothionein and proteins in general. Otvos and Armitage correctly deduced the organization of the metal-thiolate clusters in MT by selective decoupling of the ^{113}Cd NMR spectrum of $^{113}Cd_7MT$ [149]. Their structural model was reported seven years prior to the publication of the crystallographic structure, and was of central importance to MT research in the intervening years. Wuthrich and coworkers at the ETH in Zurich have employed recently developed two-dimensional ^1H techniques to provide complete sequence-specific assignments for the ^1H spectra of rabbit liver and rat liver Cd_7metallothioneins [150, 151] and construct models for the solution structures of metallothioneins [152, 153].

MT is a relatively small biopolymer and thus amenable to study by ^1H NMR. However, the signal dispersions in ^1H spectra of MT are not as great as in most other proteins due to the lack of ring currents from aromatic residues. The principle difficulties in obtaining high quality ^1H NMR spectra of proteins are the relatively low molar solubility

of proteins, the large number of resonance lines occurring within a narrow chemical shift range, and the broad line widths due to slow tumbling rates. These difficulties have been overcome to large degree by the higher fields and better probe designs of modern instruments.

The 300 MHz ^1H spectra recorded for the apo and native forms of rat liver MT-2 are shown in Figure 3-11. Because D_2O solutions were employed, the solvent-exchangeable amide protons, which resonate in the range 7-10 ppm, were not observed. The spectra of apoMT and native MT are similar in their gross features. The resonances in the region 3.8-4.6 ppm are predominantly those of the α-protons. The intense peak at ca. 3.0 ppm contains the methylene resonances of the twenty cysteine residues. The sharp singlets at 2.09 and 2.03 ppm derive from the methyl protons of the methionine residue and its N-acetyl group, respectively. An envelope of lysine δ-CH_2 resonances is centered at ca. 1.7 ppm. The methyl doublets of the alanine residues are grouped near 1.4 ppm, and those of the threonine residues near 1.2 ppm. The group of peaks near 1.0 ppm and below arise from methyl resonances of the aliphatic side chains of valine and isoleucine residues.

The spectrum of apoMT (Figure 3-11a) is practically identical to that of a mixture of the constituent amino acids [154] indicating that apoMT at low pH is essentially a random coil polypeptide with all amino acid residues sharing

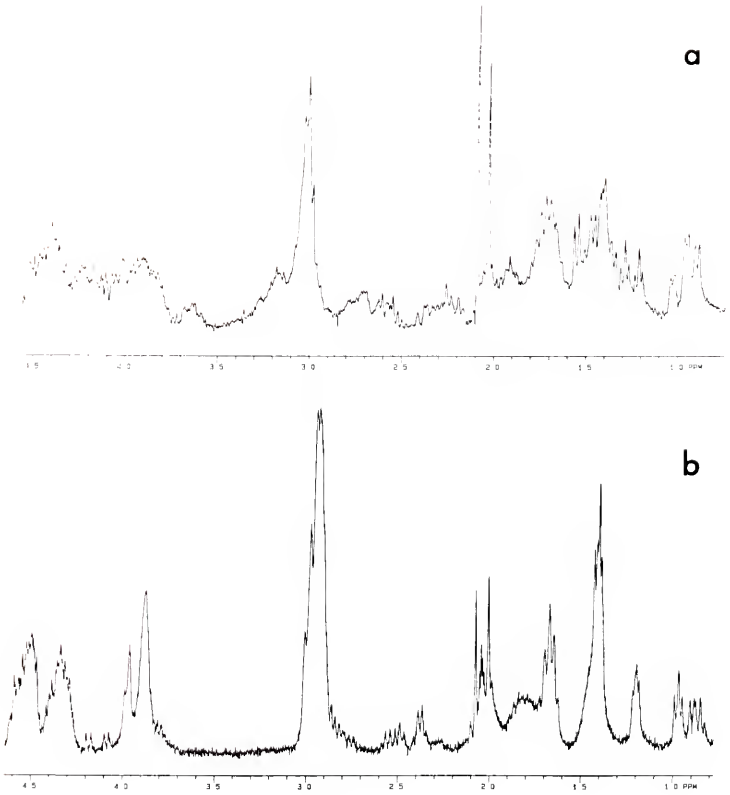

Figure 3-11. 300 MHz ^{1}H NMR spectra of (a) native rat liver MT-2 in 20 mM phosphate buffer pH 7.2 and (b) rat liver apoMT-2 in dilute acetic acid pH 2 (the multiplet at ca. 2.05 ppm, between the two sharp singlets, is from HD_2CO_2D). Resolution enhancement was employed (see Materials and Methods).

the same average environment. The spectrum of the Cd^{2+} and Zn^{2+} containing native MT (Figure 3-11b), on the other hand, shows noticeable perturbations within the resonance envelope for a particular amino acid, with the most striking effects revealed within the alanine and threonine methyl regions.

A disperse lysine δ-CH_2 proton envelope (1.6-1.8 ppm) appears in the spectrum of the folded metallated form of the protein. The lysines in apoMT, on the other hand, appear to share the same average environment and give rise to a single well defined quintet at 1.68 ppm. MT has a high proportion of lysine residues ($CH_2CH_2CH_2CH_2NH_2$ side chain), located almost exclusively adjacent to cysteines in positions which are highly conserved among the amino acid sequences of all mammalian metallothioneins (cf. Figure 1-1). Kojima [73] suggested that these lysines, which are protonated at physiological pH, serve to neutralize the net negative charge borne by the metal-thiolate clusters thereby stabilizing the molecule. Vasak, Kagi, and coworkers [155-157] have provided experimental evidence which support this type of interaction involving the lysine residues.

In the spectrum of apoMT the cysteine ß-CH_2 resonances (40 protons) centered at about 3.0 ppm overlap with ϵ-CH_2 resonances of the 8 lysines (16 protons). In the spectrum of native MT the cysteine ß-CH_2 resonances are spread out over range of about 0.5 ppm under the base of this peak [151]. However, a comparison of the area under the 3.0 ppm

peak with that of the 0.9-1.1 ppm envelope (valine and isoleucine methyls, 12 protons) confirms that the majority of the cysteine ß-CH_2 resonances are still centered at 3.0 ppm in native MT.

The chemical shifts are sensitive to the metallic elements present. Mitsumori and Tohyama [158] have shown that when the Zn^{2+} ions in native MT (67:37 Cd:Zn ratio) are displaced by Cd^{2+} ions, to form Cd_7MT, the apparent triplets at 1.2 and 1.3 ppm coalesce into two doublets. The heterogenous metal composition of native MT results in two slightly different environments for threonines 9 and 27 causing a superimposition of a pair of doublets for each residue giving the two "pseudo-triplet" shapes. The native MT sample whose spectrum appears in Figure 3-11 contained 3.18 ± 0.10 mol Zn/mol MT and the presence of bound Zn^{2+} is apparent from the pseudo-triplets of the two threonine residues.

The nature of the metal binding sites in rat liver MT-2 is revealed in a comparison of the ^1H spin-echo spectra of apoMT and native MT (Figure 3-12). Spin-echo experiments generally employ the pulse sequence 90^{o}_{x}-τ-180^{o}_{y}-τ-echo. The echo has the appearance of two free induction decays (FID's) placed back to back. The FID which follows the echo maximum may be recorded and Fourier transformed to obtain the conventional spectrum. Each peak in the resolved echo, however, is modulated at a frequency which is determined by

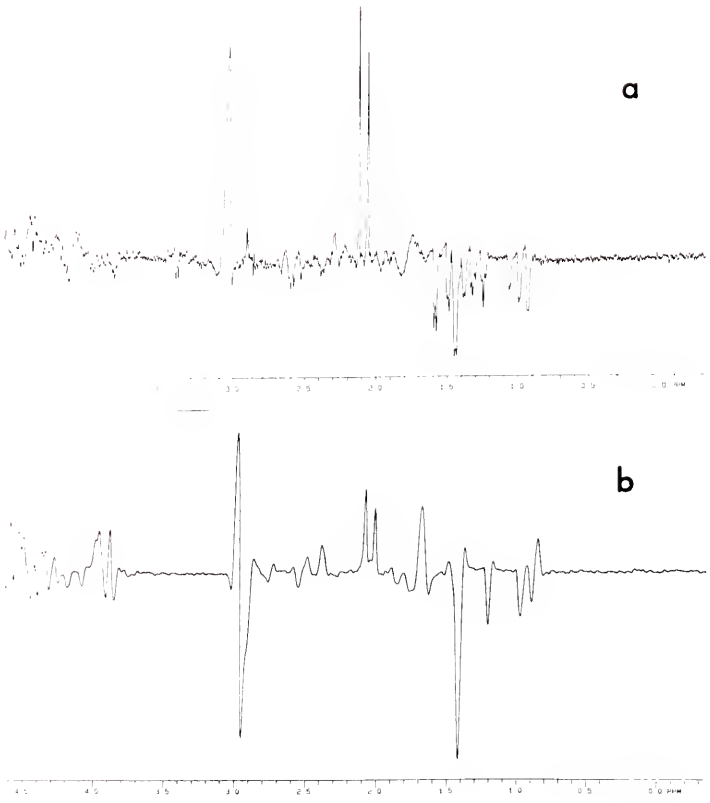

Figure 3-12. 300 MHz ^{1}H spin-echo NMR spectra of (a) native rat liver MT-2 in 20 mM phosphate buffer pH 7.2 and (b) rat liver apoMT-2 in dilute acetic acid pH 2. Resolution enhancement was employed (see Materials and Methods).

the J value of the given nucleus. The phase and amplitude of each peak in the spin-echo spectrum, then, is a function of this modulation due to spin-spin coupling and the length of τ.

Note that the phase of the cysteine ß-methylene envelope (ca. 3.0 ppm) in the spin-echo spectrum of native MT (Figure 3-12a) is reversed from that of apoMT (Figure 3-12b). The phase of a spin-echo resonance line is sensitive to spin-spin coupling [159], so coordination of metal ions to the cysteine residues must alter the coupling of these protons to each other and the cysteine α protons. The only other apparent phase reversal is for the peak farthest upfield, which is that of the methyl protons of valine 39. This is peculiar as binding of metal ions to the isopropyl side chain of this residue does not occur, but an interaction of the carbonyl oxygen or amide nitrogen with a metal ion cannot be ruled out. This spin-echo experiment was adapted from a similar experiment reported by Galdes et al. for equine kidney MT [160].

The conventional ^1H NMR spectrum and spin-echo spectrum of Pt_7MT are shown in Figure 3-13. The familiar resonance envelopes for the different amino acid spin systems, that are seen for the apo and native protein, are also found in about the same chemical shift ranges in the ^1H spectrum of Pt_7MT. Unfortunately, even very concentrated samples of Pt_7MT gave only a very weak signal. The spectrum is of

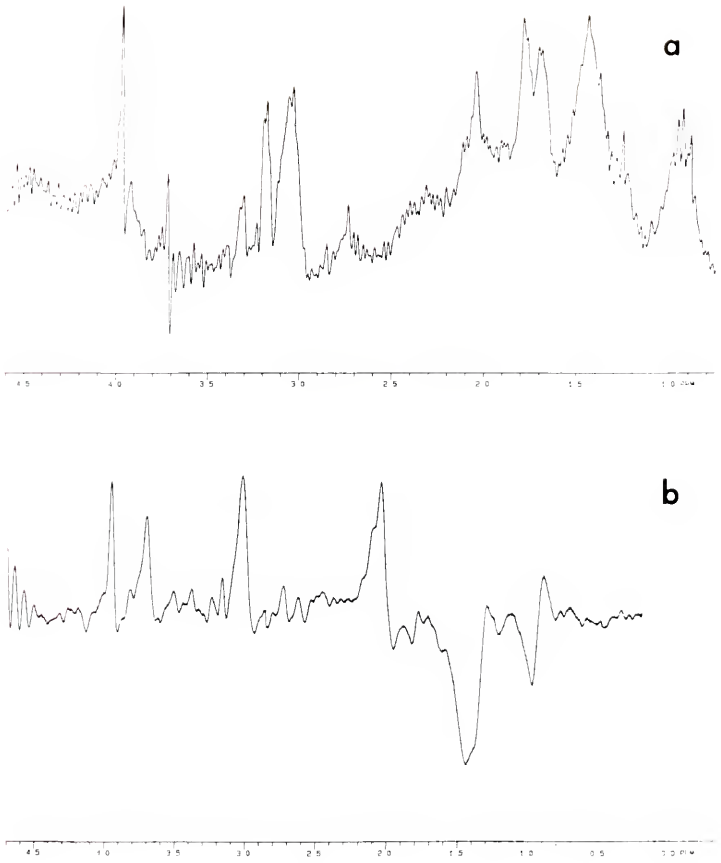

Figure 3-13. 300 MHz ^{1}H (a) NMR spectrum and (b) spin-echo NMR spectrum of 0.6 mM rat liver Pt_7MT-2 (6.96 ± 0.41 mol Pt/mol MT) in 20 mM phosphate buffer pH 7.2. Resolution enhancement was employed (see Materials and Methods).

relatively poor quality due to the low signal to noise ratio. The low S/N may be the result of heterogeneity in the binding of Pt^{2+} to individual MT apoMT molecules, slower T_1 relaxation rates due to the larger size of Pt_7MT compared to apoMT and other metal MT adducts or more restricted intramolecular motion due to Pt^{2+} binding, or some other unknown reason. A slight improvement in signal strength was obtained by using longer delay times between pulses, which indicates that relaxation processes are at least part of the problem in this case.

Coordination of the cysteine residues to ^{195}Pt (natural abundance: 32%) causes a 32% reduction the intensity of the ß-CH_2 resonances. The ^{195}Pt satellite peaks are broadened beyond detection at this high applied field as a consequence of chemical shift anisotropy [161]. The 3.0 ppm region in the spectrum of Pt_7MT (Figure 3-13a) shows very little intensity, even taking into account coupling of the cysteine CH_2 protons to ^{195}Pt. This is not necessarily due to heterogeneity in Pt_7MT binding sites, however, as these resonances are spread over a large range (ca. 0.5 ppm) in the homogeneous adduct, Cd_7MT [151].

Examination of the spectra for apoMT and native MT (Figure 3-11) reveals that the cysteine ß-CH_2 peak in the spectrum of native MT is shifted about 0.1 ppm downfield from that found for apoMT. This same deshielding effect is seen also in Figure 3-13a for Pt_7MT. What was observed as a

single broad 3.0 ppm resonance region in the spectrum of native MT occurs as three separate peaks in the spectrum of Pt_7MT. Binding of the cysteines to Pt^{2+} may cause more pronounced deshielding of some the ß-CH_2 protons than occurs with Cd^{2+} and Zn^{2+} binding. This effect is consistent with the greater electron-withdrawing tendency of Pt(II) versus Cd(II) or Zn(II), as seen in the electronic absorption spectra.

The two sharp methyl singlets from the acetylated methionine residue which appear in the other MT spectra are noticeably absent in the spectrum of Pt_7MT. There is a relatively sharp peak occurring at 2.05 ppm which can be assigned to the acetyl group methyl but the methyl resonance of met-1 is either shifted to another region of the spectrum or broadened beyond detection.

Gummin and coworkers have recently investigated the NMR properties of the complex formed between K_2PtCl_4 and N-acetylmethionine [162]. The CH_3S peak (1.96 ppm) shifts downfield by 0.31 ppm upon complexation of Pt^{2+} by the sulfur atom and splits into a "1:4:1" pattern due to ^{195}Pt coupling. The two ^{195}Pt satellites were broadened beyond detection in the 300 MHz spectrum. The methyl singlet of the acetyl group was unaffected by complexation. These results are in agreement with the earlier finding by Boswell, et. al, that upon complexation with K_2PtCl_4 the

CH_3S resonance line of this compound is shifted 0.30 ppm downfield from 2.04 ppm for the free ligand [163].

From the above results it is expected that coordination of Pt^{2+} to met-1 of MT would cause the CH_3S peak at 2.09 ppm to vanish while leaving unchanged the $CH_3C(O)$ peak at 2.03 ppm. This is exactly what is observed in the spectrum of Pt_7MT, strongly suggesting that coordination of Pt^{2+} to the thioether sulfur of met-1 does occur in this adduct. However, predicting the new location of the CH_3S peak in the spectrum of Pt_7MT is problematic. The direction and extent of the shift is dependent on the particular protein molecule in which the methionine residue resides. In the complex formed by K_2PtCl_4 and met-65 of tuna ferrocytochrome c, for example, this peak is actually removed 0.15 ppm upfield from the position of this peak in the free protein [163].

Bell and coworkers have recently examined the 500 MHz ^1H spin-echo NMR spectra of cell culture media before and after addition of K_2PtCl_4, cisplatin, and Pt(en)Cl2 [164]. They report the disappearance of the methionine CH_3S peak at 2.15 ppm and the appearance of a new peak at ca. 2.71 ppm after addition of each of the above reagents. It is interesting, in light of this report, that a fairly sharp peak is observed at 2.75 ppm in the spectrum of Pt_7MT. This peak may be that of the methionine CH_3S coordinated to Pt^{2+} but this peak may lie elsewhere in the spectrum, perhaps obscured by other resonances.

The spin-echo spectrum of Pt_7MT in Figure 3-13b is similar to that of the native protein (Figure 3-12b) in that the phases of the various resonance regions are the same. The only apparent difference is in the phase of the methyl doublet of the isopropyl side chain of valine 39 that appears farthest upfield in the two spectra. The phase of this peak is positive in the Pt_7MT and apoMT spin-echo spectra but, but as noted earlier in this section, it is negative in the native MT spectrum. The large positive cysteine 3.0 ppm peak confirms that cysteines are involved in Pt^{2+} binding.

^{195}Pt NMR appeared to be a very promising method of studying the structure of Pt_7MT at the outset of this investigation. The high natural abundance, good receptivity, and extremely large known chemical shift range of this spin 1/2 nucleus make it possible, in principle, to determine the number of distinct Pt-thiolate clusters and how the Pt^{2+} ions in these clusters are arranged by the spin-coupling in the spectrum as was done for Cd_7MT by using ^{113}Cd NMR [165, 166]. Unfortunately no ^{195}Pt signal was observed from concentrated samples of Pt_7MT using either the 200 or 300 MHz instruments. Attempts by Ismail and Sadler to observe ^{195}Pt signals from Pt^{2+} bound to other macromolecules also ended in failure, and this was attributed to relaxation by chemical shift anisotropy [167].

A similar difficulty in obtaining ^{199}Hg NMR spectra of Hg_7MT has been encountered [25].

Binding Kinetics

Unlike the intensive research activity dedicated to learning about the structures and equilibrium properties of MT adducts, the kinetics of metal binding to apoMT is an essentially unexplored area. The main reasons for this lack of interest probably include the difficulty in modeling a complex system containing multiple binding sites and the prohibitively rapid binding rates of the physiologically prevalent Cd^{2+} and Zn^{2+} ions. The extreme inertness of Pt(II) complexation can be used to advantage in this regard as it was in the previously described titration of partially platinated MT derivatives with DTNB.

Changes in the ultraviolet absorption spectrum provide a convenient albeit crude measure of the extent of reaction of K_2PtCl_4 with apoMT. The complex nature of the spectrum does not translate into a simple relationship between intensity at a given wavelength and concentration of reactants. It provides only a very rough measure of the concentration of bound Pt^{2+} ions.

Absorbance was monitored versus time at 280 nm for a micromolar solution of apoMT mixed with a 50-fold molar excess of K_2PtCl_4 at room temperature. This wavelength was

chosen as the absorption at 280 nm increases in a nearly linear fashion versus mol equiv of bound Pt(II) (Figure 3-5b). The data may be fitted as two pseudo-first-order processes to a logarithmic plot of $(A_\infty - A)$, which is proportional to the concentration of apoMT, versus time (Figure 3-14a). This treatment is consistent with either consecutive or parallel reactions leading to the formation of Pt_7MT. The plot of $\log(A_\infty - A)_I$ in Figure 3-14b was obtained by subtracting from the biphasic plot the contribution of the slow step II, i.e. $\log(A_\infty - A)_{II}$, after extrapolating step II to zero time.

One interesting observation about this treatment of the data is that the ratio of A_∞ for step I to that of step II is 0.32/0.75 = 0.43 = 3.0/7.0. The obvious interpretation is that the fast phase is the binding of the first 3 Pt^{2+} ions to the apoMT molecule, which occurs by the formation of three $Pt(cys)_4^{2-}$ moieties, and that incorporation of the remaining 4 Pt^{2+} ions, which must proceed via the formation of some bridging thiolates, is the slower step II. It is reasonable to suppose that binding of the first 3 Pt^{2+} ions would occur more rapidly due to the abundance of solvent-exposed thiolate ligands resulting from the greater freedom of motion of the loosely coiled polypeptide during the early stages of binding. The number of binding sites available to an incoming Pt^{2+} ion during the later stages of binding is

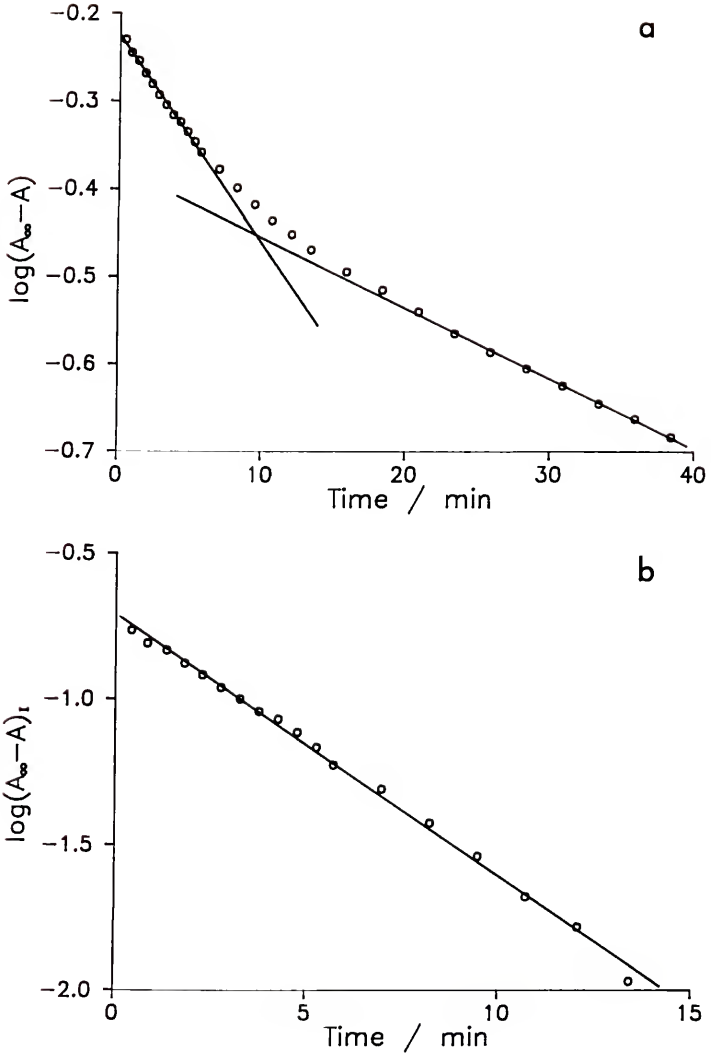

Figure 3-14. Shown are (a) the time course of the reaction of 10 μM apoMT with a 50-fold molar excess of K_2PtCl_4 in 15 mM phosphate buffer pH 7.5, and (b) the plot obtained by subtracting the contribution to the absorbance of the slow component of the reaction, A_{II}. A_∞ is the absorbance at 280 nm estimated for infinite time.

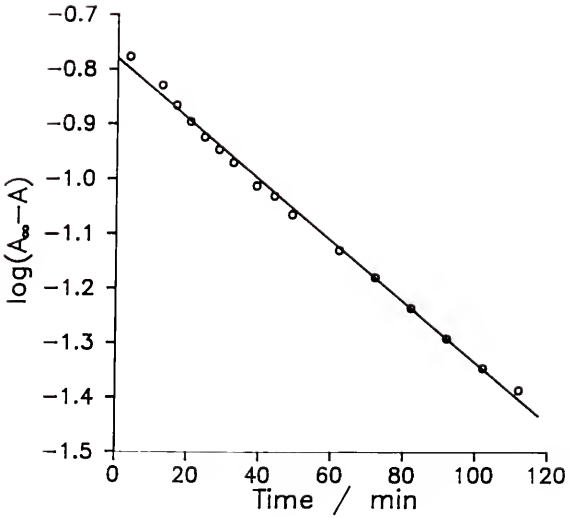

Figure 3-15. Time course of the reaction of 10 μM apoMT with a 50-fold molar excess of K_2PtCl_4 in 0.01 M HCl. A_∞ is the absorbance at 280 nm estimated for infinite time.

more restricted, on a purely statistical basis, than during the initial formation of the $Pt(cys)_4^{2-}$ units.

This interpretation assumes that the binding of each Pt^{2+} ion produces an equal increase in the absorbance at 280 nm. Of course, this assumption about the additiveness of bound Pt^{2+} absorptivities is only approximately correct as may be seen by the titration data in Figure 3-5.

The slower binding of excess Pt^{2+} to apoMT at low pH does not exhibit biphasic kinetics. The data yield a single pseudo-first-order process (Figure 3-15). As was seen in the ^1H NMR spectra, apoMT at low pH is essentially a random coil and this is reflected in the binding of roughly 17 Pt^{2+} ions per MT to form a polymeric mixture.

Conclusions

At the outset of this project it was anticipated that Pt(II) would probably form a quite stable adduct with apoMT at neutral pH. The retention of bound Pt^{2+} at very low pH was not anticipated. Nor was it expected that seven square-planar Pt(II) ions would be chelated per MT molecule, which happens to be the same stoichiometry found for Cd^{2+}, Zn^{2+}, and other divalent metals with tetrahedral stereochemistry. The apparent similarities between Pt_7MT and these other adducts, besides the stoichiometry, are somewhat surprising in light of the two very different coordination geometries.

The large Stokes' radius of Pt_7MT suggests an elongated two-domain structure similar to that of native MT. The electronic absorption and CD spectra obtained in the step-wise titration of apoMT with K_2PtCl_4 follow a pattern very similar to that reported for the titration of apoMT with $CdCl_2$ [38]. However, the large change in the CD spectrum attending the binding of the seventh Pt^{2+} ion has no analogue in the case of Cd^{2+} binding [21], and this spectral change suggests Pt^{2+} binding at the N-terminal methionine which is not a binding site for Cd^{2+}. The DTNB assays of the partially platinated apoMT samples indicate the initial formation of three $Pt(cys)_4^{2-}$ units followed by incorporation of the remaining Pt^{2+} ions in bridged metal-thiolate clusters. A similar binding sequence has been proposed for the formation of Cd_7MT [38].

That such cluster formation should occur in Pt_7MT is not surprising in view of the great propensity of classical thiol ligands to act as bridging ligands in their Pt(II) complexes. Simple thiols react with Pt(II) to form amorphous $[Pt(\mu\text{-}RS)_2]_n$ polymers (R = CH_3, CH_3CH_2, C_6H_5, etc.) [49]. The fundamental differences between Pt_7MT and adducts of apoMT with the lighter metallic elements, in addition to the different stereochemistries, are the much greater strength of the Pt^{2+} to sulfur bonds, the much slower rate of Pt^{2+} binding, and the probable binding of one the seven Pt^{2+} ions at met-1.

The process of metal ion binding at neutral pH to form the fully metallated form of MT from the apo form takes a course intermediate between two extremes. The first extreme is that of a rigid apoMT with preformed binding sites into which the metal ions are held. The second extreme is that of a random coil polypeptide that wraps around the metal thiolate complexes. ApoMT is essentially a random coil at neutral pH as its ^{1}H NMR spectrum is nearly identical to that of a mixture of the component amino acids [135]. The binding of Pt(II) to apoMT is probably a fairly random process under kinetic control. If the initial formation of $Pt(cys)_4^{2-}$ units is sufficiently faster than the subsequent phase of binding which entails thiolato bridging, as suggested by the kinetic data in Figure 3-14, it is not necessary that there be any thermodynamically favored binding sites in order for the type of spectral changes in Figure 3-5b to be observed.

It is possible, for instance, that the binding of 7 Cd(II) ions to apoMT at neutral pH is a random process producing a distribution of kinetic products followed by intramolecular reorganization of the Cd(II)-thiolate bonds to form a single homogeneous Cd_7MT as the thermodynamic product. ^{113}Cd NMR studies of Cd_7MT [39] and metal ion exchange between Cd_7MT and Zn_7MT [20] and a recent variable temperature CD study of Cd(II) binding to Zn_7MT by Stillman

and Zelazowski [22] all suggest that metal ions are mobile within a cluster.

Although the initial binding process and formation of metal-thiolate clusters to form Pt_7MT appears quite similar to those observed for adducts with Cd(II) and other metal ions, it is possible that the arrangement of Pt(II) ions among the 20 cysteine residues in the equilibrium product at room temperature differs from one molecule to the next due to the extreme kinetic inertness of Pt(II) which could prohibit the type of intramolecular rearrangement described above. The ^1H NMR spectrum of Pt_7MT (Figure 3-13a) is similar to the spectrum of native MT in its gross features but has a relatively weak signal strength even for very concentrated samples, which suggests this type of inhomogeneity. The weak ^1H NMR signal may also be a consequence of unusual relaxation properties of Pt_7MT or other unknown factors however.

It was hoped that the application of ^{195}Pt NMR would reveal the structural arrangement of these Pt(II)-thiolate clusters. This has not been realized due to unforeseen experimental difficulties. We must instead garner other small pieces of chemical and physical evidence to build a structural model. The discussion of a structural model for Pt_7MT is postponed until the end of Chapter 4, wherein additional data is presented regarding the arrangement of

Pt^{2+} ions in Pt_7MT and mixed metal Pt(II) adducts prepared via displacement of Cd^{2+} and Zn^{2+} from Cd_7MT and native MT.

Materials and Methods

General Procedures

Equine kidney MT-1A and rat liver MT-1 and MT-2 were isolated and purified according to a literature procedure [130]. ApoMT was prepared by exhaustive dialysis of the native protein against 0.01 M HCl. A small amount of the metal-chelating agent diphenylthiocarbazone in CCl_4 was suspended in the 0.01 M HCl.

All chemicals employed were reagent grade or better. Deionized water and buffer solutions were passed through a column of Chelex chelating resin to remove trace metal contaminants. Dialysis tubing (Spectrapor MW cut-off: 3500) was boiled repeatedly in deionized water and EDTA solution prior to use.

Manipulations of oxygen-sensitive materials were done in a glove-box with nitrogen atmosphere and oxygen furnace. Solutions were thoroughly degassed on a vacuum line prior to transfer to the glove-box. Absorption and CD spectra were recorded on an IBM 9430 UV-visible spectrophotometer and a Jasco J-500 spectropolarimeter, respectively.

Sephadex G-50 and G-75 size-exclusion columns were calibrated for Stokes' radius against ovalbumin (R_o =

2.73 nm), chymotrypsinogen A (2.09), myoglobin (1.88), ribonuclease A (1.64), and blue dextran (∞). R_o was plotted against ($-\log K_d$), where K_d is the elution coefficient [132]. The eluant was 3.5 mM phosphate buffer, pH 7.25, and the elution was monitored continuously by absorbance at 229 nm. Flow rate was controlled by a calibrated peristaltic pump. Protein containing fractions were concentrated by using an Amicon YM5 or YM2 ultrafiltration membrane.

Analytical Method

Elemental Analyses were done by using a Perkin-Elmer Plasma II Emission spectrometer equipped with a Perkin-Elmer Series 7000 computer. The emission lines scanned were S I 180.73 nm, Cd II 214.44, Zn I 213.86, 324.75 and Pt II 214.420 nm. All protein samples were run side-by-side with ultrafiltrate or dialysate blanks. The instrumentation and methodology are described in Chapter 2.

Preparation of Pt(II) ApoMT Adducts

Samples of Pt_7MT were prepared by adjusting solutions of apoMT in 0.01 M HCl to pH 7 with K_2HPO_4 followed by the addition of a 10 to 100-fold molar excess of K_2PtCl_4. After standing for 12 to 24 hours, the reaction mixtures were fractionated on a Sephadex G-50 or G-75 size-exclusion column, and the MT containing fractions pooled and

concentrated by using an Amicon YM2 or YM5 ultrafiltration membrane.

To study the extent of Pt binding to apoMT at low pH, solutions of apoMT in 0.01 M HCl were allowed to react with excess K_2PtCl_4 over 24 hours. The extent of binding was determined by ICP-AES after stripping off unreacted Pt^{2+} by ultrafiltration and desalting the equilibrium mixture on a size-exclusion column at neutral pH.

Binding of Pt(II) to ApoMT Modified at Methionine

The N-terminal methionine of apoMT was converted to methionine sulfoxide by using the method described by Schechter [133]. ApoMT in 1 M HCl was allowed to react with 1 M dimethyl-sulfoxide for 30 minutes. The resulting dimethyldisulfide and unreacted DMSO were removed by repeated dialysis against 0.01 M HCl. Cd(II) and Pt(II) adducts of this modified apoMT were prepared in the glove-box at neutral pH as by using the procedure described in the preceding section. The Cd(II) and Pt(II) adducts of the modified apoMT were assayed for Cd, Pt, and S by ICP-AES.

Reactions of Pt_7MT with DTNB and Iodoacetate

Buffered deaerated solutions of 3.8 μM Pt_7MT (1 mL) and freshly prepared 2.0 mM 5,5'-dithiobis(2-nitrobenzoic acid) (1 mL) were mixed in a cuvet in the glove-box. The cuvet was sealed and transferred to the sample compartment of the

UV-vis spectrophotometer and the increase in absorbance at 412 nm versus time recorded. The absorbance of a blank containing all reagents except protein was subtracted from the absorbance of the sample. The final pH was 7.4.

The extent of reaction at equilibrium was determined by passing the equilibrium mixture through an ultrafiltration membrane and then measuring the absorbance of the ultrafiltrate at 412 nm versus that of a blank. The extent of reaction was calculated using the molar absorptivity of the resulting dianion of 2-nitro-5-thiobenzoic acid, 14150 M^{-1} cm^{-1} at 412 nm [168].

The rate and extent of the reaction of 9.0 μM Pt_7MT with 1.0 mM iodoacetate were obtained at pH 7.2 by measuring the release of I^- in a stirred cell with a calibrated I^- selective electrode (Lazar Res. Lab. IS-146).

Reaction of Pt_7MT with Cyanide

1.00 mL of 35 μM Pt_7MT was dialyzed against 4.00 ml of 0.1 M NaCN in 0.1 M phosphate buffer pH 7.0 for 12 hrs during which the yellow color inside the dialysis bag was gradually lost. The Pt was found to be evenly distributed between of the contents of the bag and the surrounding solution by ICP-AES analysis. Absorption bands characteristic of $Pt(CN)_4^{2-}$ were found in the ultraviolet spectrum of the solution.

Spectrophotometric Titration of Rat Liver ApoMT-1 with Pt(II) and DTNB

A series of 3.5 μM apoMT solutions containing from 0 to 10 molar equivalents of K_2PtCl4 were prepared in the glove-box. ApoMT solutions in 0.01 M HCl were adjusted to pH 7 with K_2HPO_4 and then diluted to 0.65 mL after addition of K_2PtCl_4 increments. The reaction mixtures were left standing for three hours to equilibrate. A solution of 12 mM DTNB buffered at pH 7.5 was also prepared in the glove-box.

The equilibrium mixtures were transferred to a 1 cm cuvet which was sealed with a greased septum. A 100 μL syringe charged with 60 μL of the DTNB (5,5'-dithiobis(2-nitrobenzoic acid)) solution was then mounted atop the cuvet, with the needle protruding through the septum, using a short length of tightly fitting rubber tubing. The DTNB reagent was held aloft over the protein solution by a small dead-space. This assembly was then quickly transferred to the sample compartment of the spectrophotometer.

After recording the spectrum of the equilibrium mixture, the DTNB in the syringe was discharged into the cuvet. A spectrum was recorded one minute after mixing. The cuvet and syringe were then cleaned and returned to the glove-box and the above procedure repeated for each of the remaining samples. All spectra were recorded at slow scan speed, with air in the reference beam, and using the same

cuvet. Spectra of blanks containing all reagents except protein and K_2PtCl_4 were subtracted from sample-spectra. Free thiolate concentrations were estimated using the reported molar absorptivity of the dianion of TNB (2-nitro-5-thiobenzoic acid), 14150 M^{-1} cm^{-1} at 412 nm [168].

Titration of ApoMT with Pt(II) Followed by CD

A series of 10 μM apoMT solutions containing 0 to 10 mol equiv of K_2PtCl_4 were prepared in the glove-box. ApoMT solutions in 0.01 M HCl were adjusted to pH 7.5 with NaOH and K_2HPO_4 and then diluted to volume after addition of K_2PtCl_4 increments.

CD spectra were recorded for the samples using four labeled 1 cm cuvets sealed with greased septa. CD spectra of blanks containing all reagents except protein and K_2PtCl_4 were recorded in the four cuvets and these blank-spectra were subtracted from the corresponding sample-spectra taken in the same cuvet. Five replicate scans were recorded for each sample and blank and signal-averaged.

NMR Spectra

Samples were prepared by lyophilizing solutions of protein in dilute phosphate buffer and then dissolving the resulting solids in D_2O. This procedure was performed twice for each sample in order to remove residual HDO. The samples were then transferred to 1 mm sample tubes.

All ^1H NMR spectra were run at 22°C on a Varian VXR 300 spectrometer. Chemical shifts were referenced to external DSS (3-(trimethylsilyl)-1-propanesulfonate). The HDO signal was suppressed via T_1 discrimination, i.e. by applying a 180° pulse and 2 s delay prior to each 90° pulse. Resolution enhancement was obtained, for the spectra indicated, by weighting the FID by exp(t/K), where K ≈ 0.5, and a Gaussian apodization function.

Spin echo spectra were obtained by the Carr-Purcell method [169]. The pulse sequence 90°-τ-180°-τ-collect was used with τ = 50 ms.

Binding Kinetics

A syringe containing 80 µL of 4.95 mM K_2PtCl_4 was mounted atop a cuvet containing 720 µL of 11.1 µM apoMT buffered at pH 7.5 (50:1 molar ratio Pt:apoMT) as described above for the spectrophotometric titrations. This assembly was transferred from the glove-box to the spectrophotometer. The contents of the syringe were discharged into the cuvet and the increase in absorbance versus time at 280 nm was recorded on a strip-chart recorder.

A similar experiment was conducted for a solution of apoMT in 0.01 M HCl. ApoMT is stable with respect to air-oxidation at this pH so the manipulations were performed on the bench top.

CHAPTER 4
DISPLACEMENT OF CADMIUM AND ZINC FROM METALLOTHIONEIN BY PLATINUM(II)

The preceding chapter described experiments with simple systems consisting of solutions apoMT and K_2PtCl_4. In this chapter the more complex and biologically relevant problem of the formation of platinum(II) metallothioneins by displacement of Cd^{2+} and Zn^{2+} ions from native MT is considered. The first problem to be examined will be the reaction of K_2PtCl_4 with Cd_7MT. This is followed by a discussion of the binding of Pt(II) from K_2PtCl_4 and the derivatives of the anticancer drug, cisplatin, to heterogenous native metallothioneins, which contain predominantly Cd^{2+} and Zn^{2+} as well as lesser amounts of Cu^{+}. The results presented in Chapter 3 for the binding of Pt(II) to apoMT are used in an attempt to understand the adducts obtained by displacement of metal ions from the above adducts and a structural model for Pt(II)-thiolate clusters is described. Finally, implications for the metabolism of cisplatin *in vivo* are outlined.

Reactions of Native and Cadmium Metallothioneins with Tetrachloroplatinate

An experiment involving reactions of K_2PtCl_4 with Cd_7MT gave somewhat unexpected results [27]. Our original intention was to attempt to produce Cd_7MT with a single Pt^{2+} bound to the thioether sulfur of the N-terminal met-1 residue. We assumed that the Cd^{2+} ions in Cd_7MT were bound strongly enough to prevent the Pt^{2+} ions from reacting with the cysteine residues. It was found, however, that the addition of one mol equiv of K_2PtCl_4 or a slight molar excess of K_2PtCl_4 resulted in the liberation of 3 mol equiv of Cd^{2+} ions from Cd_7MT (Table 4-1). In the presence of air a single Pt^{2+} ion was bound whereas in the exclusion of air 4 Pt^{2+} ions were bound to produce a Pt_4Cd_4MT.

The retention of 4 mol equiv of Cd^{2+} ions in all the above cases strongly suggests that Pt(II) is displacing Cd^{2+} from the 3-Cd ß cluster and leaving the 4-Cd α cluster intact. This result is a reasonable one as Cd^{2+} shows a marked preference for the α cluster in native MT and tends to accumulate in this cluster as opposed to the more weakly bound Zn^{2+} which occupies the ß cluster almost exclusively. Furthermore, it is known that the ß cluster region in Cd_7MT and native MT is susceptible to attack by the strong electrophiles DTNB and iodoacetamide while the α region are generally inaccessible to these reagents [37].

Table 4-1. ICP-AES of the Products From Reactions of Cd_7MT and Native Equine MT with K_2PtCl_4.

Reactants (conditions)[a]	Metal Contents of Products	
	Metal	Mol/Mol MT[b]
5.5 μM Cd_7MT + 5.8 μM K_2PtCl4 (in air)	Cd	3.82 ± 0.87
	Pt	1.11 ± 0.25
	total	4.93 ± 0.91
8.2 μM Cd_7MT + 85 μM K_2PtCl_4 (in air)	Cd	4.01 ± 0.12
	Pt	1.16 ± 0.04
	total	5.17 ± 0.13
6.9 μM Cd_7MT + 55 μM K_2PtCl_4 (under nitrogen)	Cd	4.28 ± 0.25
	Pt	3.71 ± 0.22
	total	7.99 ± 0.33
native MT	Cd	5.04 ± 0.36
	Zn	0.94 ± 0.08
	Cu	0.63 ± 0.23
	total	6.61 ± 0.43
28 μM native MT + 990 μM K_2PtCl_4 (under nitrogen)	monomeric products	
	Cd	3.33 ± 0.49
	Zn	0.25 ± 0.10
	Cu	0.94 ± 0.21
	Pt	3.62 ± 0.42
	total	8.14 ± 0.69
	oligomeric products	
	Cd	5.04 ± 0.55
	Zn	0.18 ± 0.11
	Cu	0.10 ± 0.14
	Pt	5.27 ± 0.53
	total	10.59 ± 0.78

[a] All reactions mixtures were at pH 7.2, room temperature.

[b] (mean of sample - mean of blank) ± (standard deviation) for 6 replicate measurements of both sample and blank.

Templeton and coworkers have found that ^{113}Cd NMR lines attributed to Cd^{2+} ions in the ß cluster are lost before those attributed to Cd^{2+} ions in the α cluster during the displacement of Cd^{2+} from Cd_7MT by mercuribenzoate [170].

Rapid air oxidation of cysteine to cystine disulfide apparently occurs during the disruption of the ß cluster by entering Pt^{2+} ions. The ultraviolet spectrum of the product has absorption in the region 250-320 nm that is much too intense to be accounted for by the metal chromophores alone. Some of this absorption must arise from cystine disulfide groups which have absorption maxima at 270-280 nm. This oxidation of the cysteine side chains would abolish metal binding in this cluster. The single mol equiv of Pt^{2+} which is found in the final product is probably bound to the thioether sulfur of met-1, which does not undergo air-oxidation under these conditions. The reaction of Pt^{2+} ions with the cysteine sulfurs must be much faster than the reaction with methionine sulfur as the Cd^{2+} ions are lost and oxidation of the cysteines occurs even for the equimolar mixture of K_2PtCl_4 and Cd_7MT.

The reaction of excess K_2PtCl_4 with Cd_7MT under nitrogen to produce Pt_4Cd_4MT suggests that the ß cluster region can accommodate 3 Pt^{2+} ions, assuming that the remaining Pt^{2+} is bound to met-1. Extending this line of reasoning, the arrangement of Pt^{2+} ions in Pt_7MT may be that

of two separate 3Pt-thiolate cluster regions with the seventh Pt^{2+} ion bound at the methionine.

The products from the anaerobic reaction of excess K_2PtCl_4 with native MT were divided about equally between an oligomeric fraction and a monomeric fraction when chromatographed on a size exclusion column. The Stokes' radius of the monomeric products is 0.2 nm larger than that of original native MT, i.e. the same as that of Pt_7MT (ca. 1.8 nm). The oligomeric fraction was composed of a large dimer peak and progressively smaller trimer, tetramer, and higher oligomer peaks, which were pooled for analysis by ICP-AES (Table 4-1). The monomeric products show a 75% deficiency in Zn content but only a 35% deficiency in Cd content as compared to the native MT used as starting material. This result is consistent with displacement of metal ions occurring predominantly in the ß cluster as it is known that Zn^{2+} ions are localized in this region of the native protein. The metal contents of the monomeric fraction are similar to those obtained for the anaerobic reaction of Cd_7MT with K_2PtCl_4. In both cases 4 mol equiv of Pt^{2+} ions are gained and 3 mol equiv of the initially bound metal ions are lost.

The metal contents of the oligomeric fraction are quite different than those found for the monomeric fraction. The total mol metal/mol MT is very high and although most of the Zn^{2+} has been displaced, none of the Cd^{2+} is lost. The high

content of total bound metals suggests that extensive disruption of the usual metal cluster structure and conformation of MT has occurred in this fraction. Such a catastrophic structural change could certainly make the affected MT molecules susceptible to oligomerization via intermolecular S-Pt-S cross-linking. The relatively high concentrations of the reactants and the large excess of K_2PtCl_4 employed may also promote the formation of oligomeric species.

Examination of the data in Table 4-1 also reveals that while a net loss of Zn^{2+} and, to a lesser extent, Cd^{2+} occurs, essentially all of the Cu originally bound by native MT is retained in the products. It is also interesting that nearly all of this Cu ends up in the monomeric fraction of the products. It is known that Cu is more tightly bound by MT than Cd^{2+}, presumably as Cu(I) [41]. Studies by Winge and coworkers indicate that Cu^+ is preferentially bound by the ß cluster region of MT [32] as originally suggested by Briggs and Armitage [171]. It is possible that those molecules of native MT in which the metal ions occupying the ß cluster are all or nearly all Cu^+ ions are much less reactive with Pt(II) due to the presence of very tightly bound Cu(I). The results in Table 4-1 are consistent with this proposition but the Cu concentrations in the native MT employed are rather small relative to the experimental errors in the ICP-AES data.

Reactions of Native Metallothioneins with Cisplatin Derivatives

The analytical data obtained for the reactions of Cd_7MT and native MT with K_2PtCl_4 strongly suggest that Pt(II) is preferentially displacing metal ions from the ß clusters of these reactants. It is desirable, however, to obtain spectroscopic data from which precise structural information about the protein molecule can be derived. The use of ^1H NMR spectroscopy and the complete set of assignments available for native rat liver MT-2 [151] provide this opportunity. Changes in the resonance lines of individual amino acid residues of MT in the upfield region of the ^1H NMR spectrum of rat liver MT-2 ten minutes following the addition of excess cis-$Pt(NH_3)_2(NO_3)_2$ are shown in Figure 4-1. This derivative was used instead of cisplatin because of the prohibitively low solubility of the latter.

Note that the resonance lines of residues 8, 9, and 27, all of which lie in the ß domain of MT (residues 1-29), are significantly broadened during the early stages of the reaction while the lines of residues in the α (residues 30-61) domain are relatively unaffected. This confirms that Pt(II) is preferentially displacing metal ions from the ß cluster as originally suggested by the analytical data.

The changes in the upfield region of the spectrum and a slight decrease in the intensity of the cysteine ß-CH_2 line

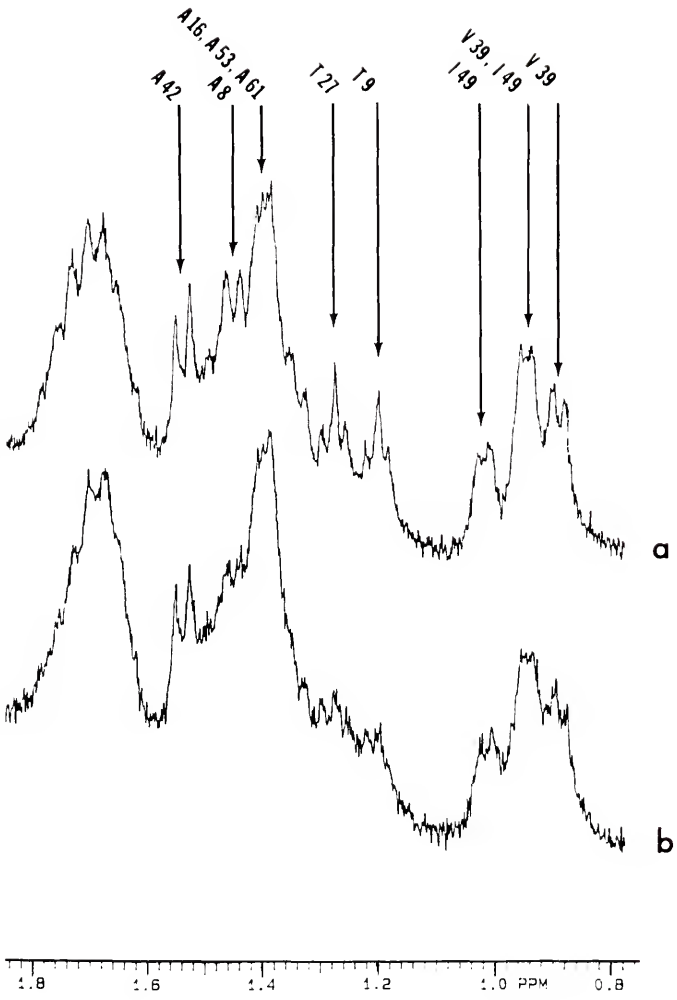

Figure 4-1. 300 MHz ^{1}H NMR spectra of (a) 0.33 mM native rat liver MT-2 in 20 mM phosphate buffer pH 7 and (b) the same sample 10 min after the addition of a 20-fold molar excess of cis-$Pt(NH_3)_2(NO_3)_2$. Selected resonance lines are labeled with the names of the amino acid residues from which they arise.

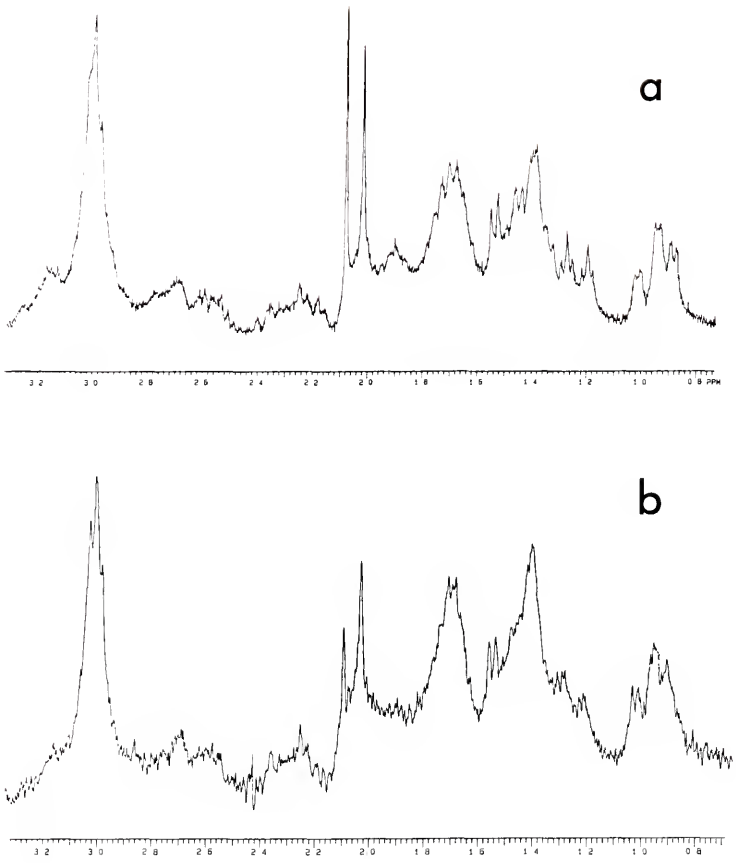

Figure 4-2. 300 MHz ^{1}H NMR spectra of (a) 0.33 mM native rat liver MT-2 in 20 mM phosphate buffer pH 7 and (b) the same sample 12 hrs after the addition of a 20-fold molar excess of <u>cis</u>-$Pt(NH_3)_2(NO_3)_2$.

(ca. 3.0 ppm) occur quite rapidly after mixing the reactants. There is also a change in the N-terminal methionine methyl peak (2.09 ppm) that occurs over a longer time period. Figure 4-2 shows the full spectrum before and 12 hours following addition of the Pt reagent. The 2.09 ppm line experiences a noticeable broadening over the 12 hrs. The methyl peak of the N-acetyl group attached to met-1 (2.03 ppm) also shows some broadening, but to a lesser extent than the met-1 methyl peak.

A slight decrease in the ratio of signal-to-noise (S/N) occurs over 12 hrs (the spectra in Figures 4-1 and 4-2 were not altered by weighting of the FID). This overall degradation of spectral quality is due to the formation of oligomeric MT species and colloidal zinc hydroxides during the reaction. The methyl singlets at 2.03 and 2.09 ppm are both very liable to broaden due to overall loss of S/N because of their narrow line widths. The greater change which occurs to the 2.09 ppm line versus the 2.03 ppm line suggests, however, that Pt^{2+} binding to met-1 may also be partly responsible for the broadening of this line.

Figure 4-3 shows the elution profile of this reaction mixture on a size-exclusion column. The products were recovered as 50% monomers, 15% dimers, and 35% higher oligomers. The average Stokes' radius of the monomeric fraction is similar to that of Cd_7MT and native MT (1.60 nm). Table 4-2 shows the analytical data obtained for

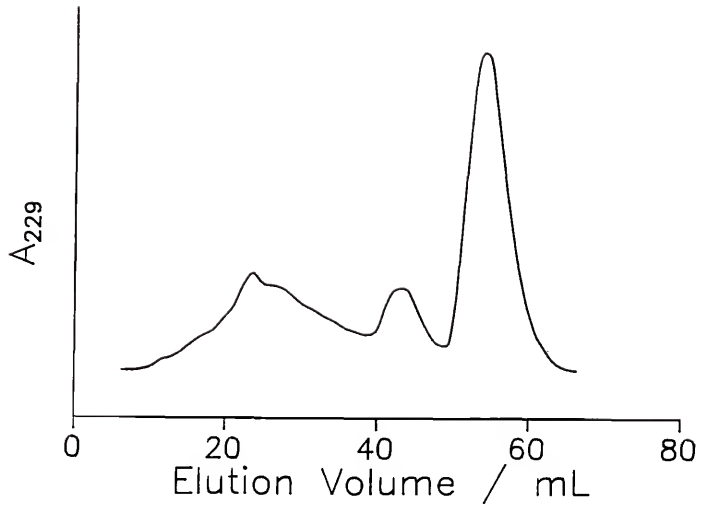

Figure 4-3. Elution profile of the products from the reaction of native rat liver MT-2 with excess $Pt(NH_3)_2(NO_3)_2$ fractionated on a Sephadex G-50 size-exclusion column. A_{229} is the absorbance at 229 nm.

Table 4-2. ICP-AES of Products From the Reaction of Native Rat Liver MT-2 with cis-$Pt(NH_3)_2(NO_3)_2$.

Reactants (conditions)	Metal Contents of Products	
	Metal	Mol/Mol MT[a]
native MT-2	Cd	3.02 ± 0.15
	Zn	3.18 ± 0.10
	Cu	0.26 ± 0.03
	total	6.46 ± 0.18
0.28 mM native MT-2 + 7.1 mM cis-$Pt(NH_3)_2(NO_3)_2$ (in air, pH 7.2, 25°C)	monomeric products	
	Cd	3.65 ± 0.42
	Zn	0.08 ± 0.07
	Cu	0.69 ± 0.25
	Pt	1.13 ± 0.28
	total	5.55 ± 0.57
	dimeric products	
	Cd	0.32 ± 0.20
	Zn	0.63 ± 0.24
	Cu	1.96 ± 0.64
	Pt	3.34 ± 0.92
	total	6.25 ± 1.17
	oligomeric products	
	Cd	0.48 ± 0.81
	Zn	2.04 ± 1.67
	Cu	0.38 ± 2.57
	Pt	0.67 ± 2.62
	total	3.57 ± 4.11

[a] (mean of sample - mean of blank) ± (standard deviation) for 6 replicate measurements of both sample and blank.

the three fractions. The metal contents of the monomeric fraction are consistent with displacement of metal ions occurring exclusively in the zinc-rich ß cluster of native MT. Nearly 4 mol Cd/mol MT are retained in this fraction and 1 mol Pt/mol MT is bound. These data are nearly the same as those obtained for the aerobic reaction of Cd_7MT with excess K_2PtCl_4.

The metal contents of the dimeric fraction differ greatly from those of the monomeric fraction. Much less bound cadmium is present and the values for bound Pt and total bound metals are both much greater. The bound Cu contents of the monomeric and dimeric products are significantly higher than the Cu content in the starting material. Unfortunately the ICP-AES data obtained for the oligomeric fraction are of very poor quality and thus a mass balance cannot be obtained for Cu as was done for the anaerobic reaction of native MT with excess K_2PtCl_4.

The monomeric fraction was also tested for the presence of disulfide bonds by using the colorimetric reagent 2-nitro-5-thiosulfobenzoate (NTSB) [172]. Shown in Figure 4-4 is the cleavage of a disulfide by sulfite, followed by attack of NTSB on the resulting thiolate to yield the highly colored dianion of 2-nitro-5-thiobenzoic acid (TNB^{2-}). Two such assays on the monomeric fraction found ca. 3-4 mol disulfide/mol MT. This is close to what would be expected for the oxidation of

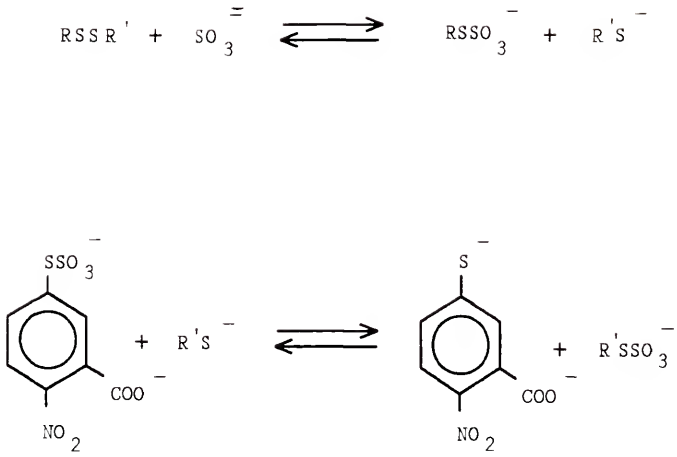

Figure 4-4. Cleavage of disulfide by sulfite followed by reaction of the resulting thiolate with TNBS.

cysteine side chains in the ß cluster to cystine disulfides. It is possible that the NTSB undergoes an unwanted reaction with the metal-bound thiolates in the α cluster, thus giving a false analytical result. However, if these thiolates were not sufficiently protected from NTSB by the bound metal ions, one would expect a much larger production of TNB^{2-} than actually found.

The sulfur donor ligands, thiolates and thioethers, are known to have high trans-labilizing effects in Pt(II) complexes [49]. Thus, the binding of cis-diammine Pt(II) complexes to native MT should involve the loss of amine ligands via trans-labilization and the ultimate products would be the same as would be obtained from the binding of $PtCl_4^{2-}$ under the same conditions. The following experiments were designed to test whether or not such loss of amine occurs.

The binding to native equine kidney MT of Pt from the spin labeled complex, cis-$Pt(ATMPO)_2Cl_2$ (ATMPO = 4-amino-2,2,6,6-tetramethylpiperidin-1-oxyl) [173], was followed by EPR spectroscopy. Free ATMPO ligand is readily distinguished from Pt(II) bound ATMPO by the difference in the EPR line shapes of this stable nitroxyl radical in the two states (Figure 4-5). Two broad bands occur between the central and low-field lines in the EPR spectrum of the Pt(II) complex due to electronic exchange between the two spin-labeled ligands located cis to one another.

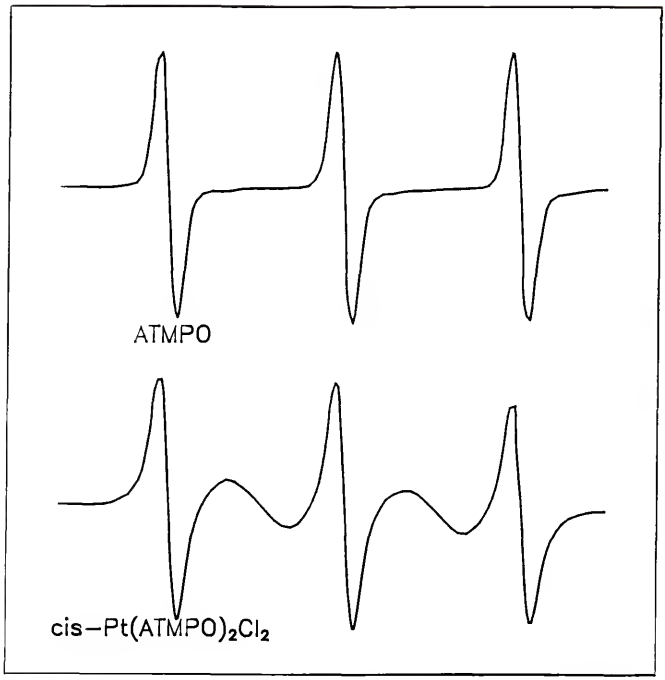

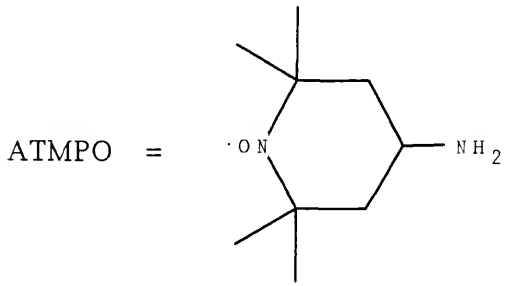

Figure 4-5. EPR line shapes of <u>cis</u>-$Pt(ATMPO)_2Cl_2$ and the ATMPO ligand in aqueous solutions.

Figure 4-6 shows the distribution of metal ions in the size-exclusion chromatographic separation of the reaction mixture as determined by high-temperature-graphite-furnace atomic absorbance spectrometric (HTGF AAS) analysis of the fractions. The reaction mixture of native MT and cis-$Pt(ATMPO)_2Cl_2$ (1:1 molar ratio Pt:MT) was kept at 37 ^{o}C for 12 hours before separation. Nearly all the original MT was recovered in the prominent monomeric fraction. The Cd to Zn ratio in the most concentrated fraction (ca. 80 mL elution volume) is approximately the same as that of the starting material suggesting that no loss of Cd^{2+} or Zn^{2+} has occurred. The ratio of the sum of Cd and Zn concentrations to the Pt concentration in this fraction is 24.6 μM/3.3 μM = 7.5. This ratio strongly suggests that a single Pt^{2+} is bound for each MT. As apparently no displacement of Cd^{2+} or Zn^{2+} has occurred, this Pt^{2+} is probably bound to the thioether sulfur of met-1.

It is evident from the data in Figure 4-6 that a small portion of the Pt (ca. 24%) did not bind to MT and was recovered in the low molecular weight fractions (120-150 mL elution volume). The total Pt recovered, as determined by AAS of the fractions, was 82 nmol. This accounts, within the limits of experimental error, for the 76 nmol of Pt complex used as starting material, also determined by AAS. The total MT recovered, as determined by AAS of Cd and Zn, was 55 nmol as compared to the 75 nmol of starting material,

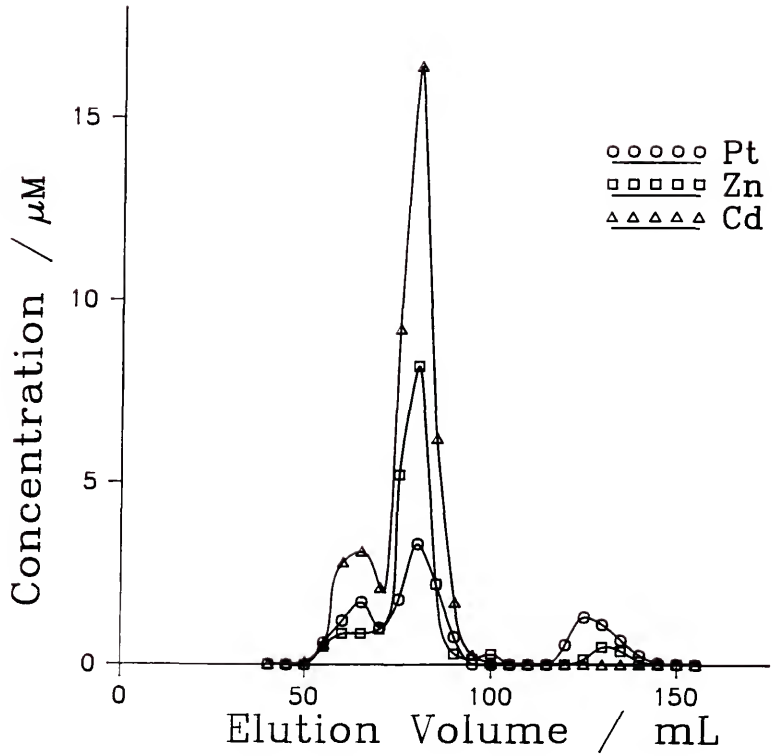

Figure 4-6. Elution profile on a Sephadex G-75 size-exclusion column of the products from the reaction of 0.13 mM native equine kidney MT with 0.13 mM cis-$Pt(ATMPO)_2Cl_2$ in 3.6 mM Tris/HCl buffer pH 7.7. Metal concentrations of the 5 mL fractions were determined by HTGF AAS.

determined gravimetrically. This apparent loss of MT (ca. 27%) is probably not an actual loss of protein during the reaction but, rather, arises from an over-estimation of the amount of MT used as starting material. This experiment was done before the ICP-AES instrumentation was in place and simple gravimetry tends to give over-estimates of total protein due to water and salts trapped in lyophilized protein samples. The mass balance, then, also shows the binding of approximately 1 mol Pt/mol MT.

Examination of EPR signals from both the protein fractions and the low MW fractions indicated that extensive loss of spin-labeled amine did indeed occur during the reaction. The most concentrated low MW fraction had a strong three-line EPR spectrum characteristic of the free ligand. Although about 75% of the available Pt was recovered in the protein-containing fractions, the most concentrated fraction in this region had only an extremely weak EPR signal which was visible above the background noise only at an amplification forty-times that used for the low MW fraction. A blank containing all reagents except MT was also kept at 37^{o}C for 12 hours and no loss of amine from the spin-labeled Pt(II) complex was observed.

Figure 4-7 shows results from a similar experiment wherein the amount of MT was one fourth that used in the previous experiment (4:1 molar ratio Pt:MT). It is interesting that, with excess Pt complex present in the

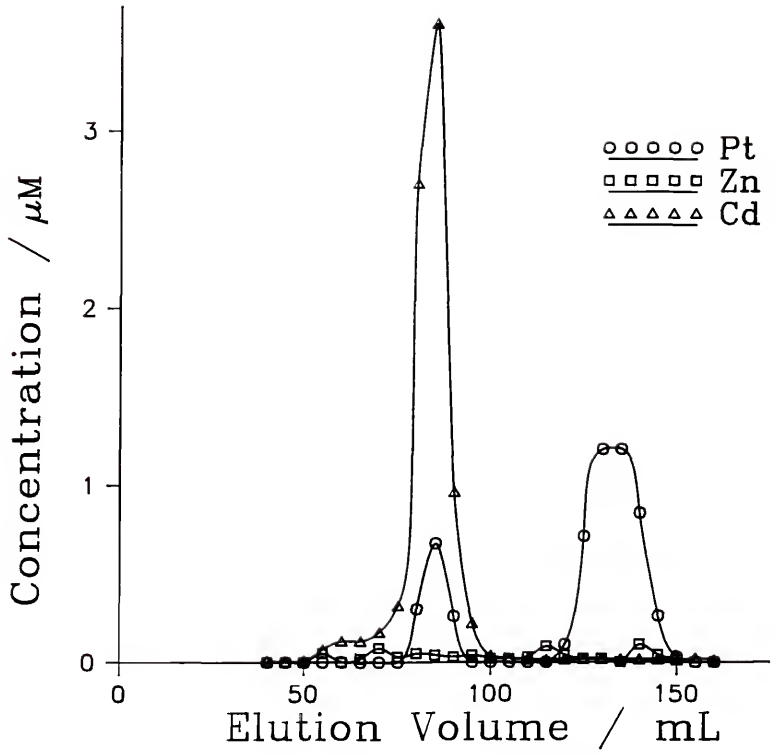

Figure 4-7. Elution profile on a Sephadex G-75 size-exclusion column of the products from the reaction of 0.04 mM native equine kidney MT with 0.16 mM cis-$Pt(ATMPO)_2Cl_2$ in 3.6 mM Tris/HCl buffer pH 7.7. Metal concentrations of the 5 mL fractions were determined by HTGF AAS.

reaction mixture, all of the Zn^{2+} originally present in the MT is liberated. The Zn^{2+} lost from MT precipitated as a gelatinous hydroxide and was not recovered in the low MW fraction. The ratio of Cd to Pt in the most concentrated MT-containing fraction is 3.6 μM/0.7 μM = 5.1, nearly the same ratio that was obtained in the 1:1 Pt:MT experiment (16.4 μM/3.3 μM = 5.0). This suggests that, again, no Cd^{2+} was displaced and that a single mol Pt/mol MT was bound. The ratio of free Pt recovered versus bound Pt recovered (ca. 3.4) also supports this conclusion.

The EPR spectra observed for the fractions from the 4:1 Pt:MT experiment were the same as those obtained in the 1:1 Pt:MT experiment. A strong three-line EPR spectrum, characteristic of the free amine ligand, was again found for the most concentrated low MW fraction and the most concentrated MT-containing fraction had only a very weak signal.

Ismail and Sadler [167] have also observed trans-labilization of amine ligands in reactions of cis-diamminedichloro complexes of Pt(II) with N-acetyl-methionine, glycine-methionine dipeptide, and RNase A. Release of both coordinated NH_3 and ethylenediamine was observed via ^{15}N NMR.

The reactivity of $Pt(ATMPO)_2Cl_2$ with native MT is similar to that of K_2PtCl_4 with Cd_7MT except that no displacement of metal ions from the MT occurred in the 1:1

$Pt(ATMPO)_2Cl_2$:MT reaction mixture despite reactant concentrations about twenty times greater than in the 1:1 K_2PtCl_4:Cd_7MT mixture and the higher temperature. The lower reactivity of $Pt(ATMPO)_2Cl_2$ may be due to the bulky ATMPO ligands preventing the complex from penetrating into the metal clusters of the MT molecule. The difference in charge between the neutral spin-labeled complex and the tetrachloroplatinate ion may also be important in the absence of extensive hydrolysis.

Conclusions

The experimental results described in Chapter 3 provide evidence that, despite the square planar geometry of Pt(II), thiolato-bridged Pt^{2+} clusters exist in Pt_7MT that are similar to the clusters in other metal MT adducts. Experiments described in this chapter provide information about the distribution of Pt^{2+} ions along the protein chain and the reactivity of cisplatin, and analogous Pt anticancer drugs, with MT in vitro. These limited data do not provide a final all-encompassing model for the various Pt(II) metallothioneins, but the evidence can be assembled into a partial model.

An interpretation of the binding experiments is diagrammed in Figure 4-8. Note that native MT has been represented as an idealized Cd_4Zn_3MT for the sake of

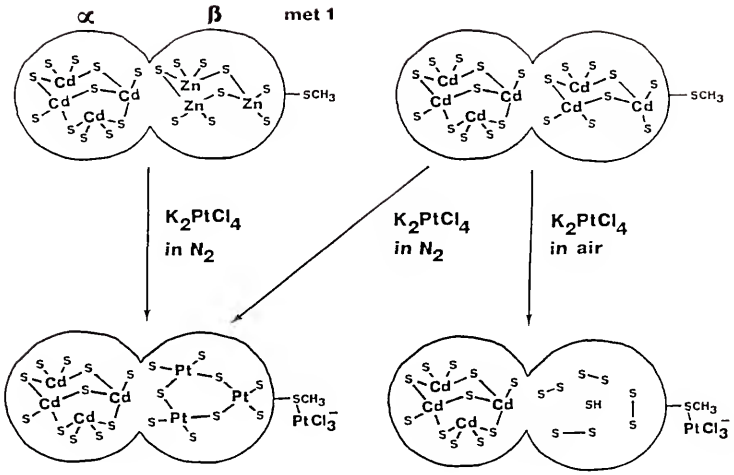

Figure 4-8. Possible products from the reactions of K_2PtCl_4 with Cd_7MT and native MT. Note that the distribution of Cd and Zn in the native MT shown above is only one of many possible distributions.

simplicity. Native MT is actually heterogenous with respect to the distribution of Cd^{2+} and Zn^{2+} ions and usually contains smaller amounts of other metal ions such as Cu^{+}, Fe^{2+}, and Pb^{2+}. The interpretation in Figure 4-8 is drawn from the following observations:

(1) Displacement of metal ions by Pt(II) occurs exclusively in the ß cluster region, as evidenced by the extensive loss of Zn^{2+} from native MT upon reaction with excess K_2PtCl_4, cis-$Pt(NH_3)_2(NO_3)_2$, and $Pt(ATMPO)_2Cl_2$. It is known that Zn^{2+} is concentrated in this region of native MT, whereas Cd^{2+} is concentrated in the α cluster [165]. It has also been shown that the ß region of fully metallated MT will react with strong electrophiles such as DTNB and iodoacetamide while the α region is kinetically inaccessible to these reagents [37]. This supposition is also consistent with the retention of four Cd^{2+} ions in the monomeric products of the reactions of K_2PtCl_4 with Cd_7MT and with native MT and the reaction of cis-$Pt(NH_3)_2(NO_3)_2$ with native MT.

(2) One mole equiv of Pt(II) binds to the N-terminal methionine residue as evidenced by the binding of a single mol equiv of Pt^{2+} to air-oxidized MT from the aerobic reaction of K_2PtCl_4 with Cd_7MT and from the aerobic reactions of cis-$Pt(NH_3)_2(NO_3)_2$ and $Pt(ATMPO)_2Cl_2$ with native MT. The cysteine thiolates are susceptible to air-oxidation, whereas the thioether side chain of methionine is

not air-oxidizable. This conclusion is further supported by the decreased binding of Pt^{2+} to apoMT containing methionine sulfoxide in place of methionine, and the disappearance of the 2.09 ppm methyl singlet of methionine in the ^{1}H NMR spectrum of Pt_7MT via coupling to ^{195}Pt. The binding of Pt(II) to the methionine of MT is not surprising because of the well known propensity of Pt(II) complexes to bind to exposed methionine residues in proteins [47, 50].

(3) If displacement of metal ions occurs exclusively in the ß cluster, and one of the four mol equiv of Pt^{2+} ions found in the monomeric products of the anaerobic reactions of K_2PtCl_4 with Cd_7MT and native MT is bound to methionine, then three mol equiv of Pt^{2+} are bound in the ß cluster region. It is likely that the same 3-Pt ß cluster in the mixed metal Cd_4Pt_4MT adduct is also present in Pt_7MT

A hypothetical 3-Pt ß cluster is depicted in Figure 4-9b. The Pt-S bond distances in Pt(II) metallothioneins should be about the same as Zn-S bond distances of MT bound Zn^{2+} ions (ca. 0.23 nm) based on crystallographic data for small thiolate containing Pt(II) complexes [174, 175]. Pt^{2+} thiolate clusters are not, however, expected to be isomorphic with tetrahedral Cd^{2+} and Zn^{2+} thiolate clusters as significant distortion of square-planar geometry around Pt(II) in these adducts is not likely to be energetically feasible. The S-Pt-S and Pt-S-Pt bond angles in Figure 4-9b are an idealized 90^{o} and 110^{o} respectively and all bond

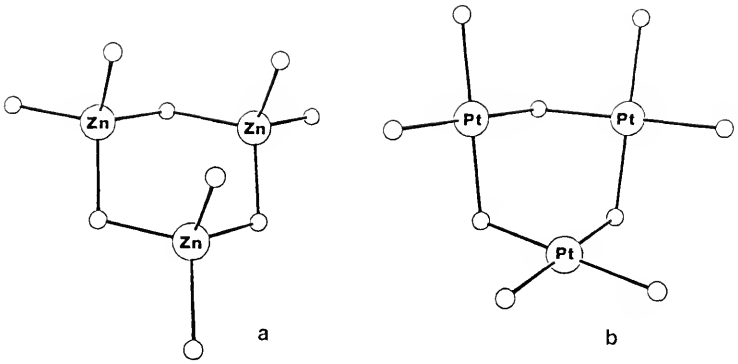

Figure 4-9. Shown are (a) the 3-metal ß cluster of native MT and (b) a hypothetical 3-Pt ß cluster. Larger circles represent metal centers; smaller circles are thiolate sulfur positions.

angles are 110^{o} in the idealized 3-Zn ß cluster (Figure 4-9a).

This particular structural model was chosen because it is easily incorporated into the crystallographic conformation found for native MT (Figure 1-2). We have found, through the use of molecular models, that only very slight changes in this conformation of the protein are needed to insert the proposed 3-Pt cluster in place of the 3-Zn cluster. The three metals and the three bridging sulfurs in the two clusters can be almost exactly superimposed upon one another, thus the only significant difference between the two structures is in the orientations of the terminal sulfurs.

The approximate differences in the orientations of these terminal ligands in going from the 3-Zn to the 3-Pt cluster are 90^{o} about the S_4 rotation-reflection axes bisecting the plane of each Zn^{2+} and its two terminal ligands. Despite the different orientations of the terminal sulfurs, this 3-Pt cluster can be inserted into the ß region of the crystallographic MT structure, without significantly changing the conformation of the polypeptide backbone, by rotations about C^{α}-C^{β} bonds of the nine cysteines in this region.

A better fit may be obtained by permitting changes in the Pt-S-Pt bond angles from the idealized 110^{o}. According to a recent review by Dance [176], bonds angles

for M-S-M bonds in metal-thiolate complexes generally vary between about 90-120°. Refinement of the crystallographic structure in Figure 1-2 from 230 to 190 pm resolution has revealed that the M-S-M bond angles in native MT actually vary from 80-130° [9]. In addition, the net forces of hydrogen-bonding and other weak interactions in the polypeptide backbone of MT probably cause slight distortions from D_{4h} about the Pt(II) centers.

Low molecular weight Pt(II)-thiolate complexes containing the structural unit in Figure 4-9b are not known, and this is not surprising as Pt(II) reacts with simple thiols to form $[Pt(\mu\text{-}SR)_2]_n$ polymers. Two Pt_3S_3 rings do occur in a hexanuclear complex of Pt(II) with 2-amino-ethanethiol, recently isolated by Gibson and Lippard [175]. In addition, the thiolato bridged trimers, $Pd_3(\mu\text{-}SC_2H_5)_3(S_2CSC_2H_5)_3$ [177] and $Pd_3(SCH_2CH_2SCH_2CH_2S)_3$ [178], both adopt structures of the type shown in Figure 4-9b.

If the $Pt_3(Cys)_9^{3-}$ in Figure 4-9b occurs in Pt_7MT for the nine cysteines in the ß region of MT, and a single Pt^{2+} ion in Pt_7MT is bound to methionine, that leaves three Pt^{2+} ions and eleven cysteines in the MT α region to be accounted for. Binding of 3 Pt^{2+} ions in this region involving all 11 cysteines would require the presence of a $(cys)_3Pt(\mu\text{-}cys)Pt(Cys)_3^{3-}$ unit and a $Pt(cys)_4^{2-}$ unit. The residual reactivity of approximately 2 mol cys/mol MT with DTNB for

Pt_7MT (Figure 3-6) suggests that a $Pt_3(cys)_9^{3-}$ cluster might also occur in the α region of Pt_7MT leaving two unbound cysteines in this region of the protein.

Materials and Methods

Reaction of K_2PtCl_4 with Cd_7MT in Air

1.1 mL of 16.3 μM K_2PtCl4 was added to 2.0 mL of 8.56 μM equine kidney Cd_7MT in 3.5 mM phosphate buffer, pH 7.2 (1:1 molar ratio Pt:Cd_7MT). After standing for 20 hrs, the reaction mixture was diluted to 20 mL and then concentrated by ultrafiltration. The resulting solution and ultrafiltrate blank were assayed for S, Cd ,and Pt by ICP-AES. A similar experiment was conducted with a reaction mixture containing 1.5 mL of the above Cd_7MT solution and 60 μL of a 2.2 mM solution of K_2PtCl_4 (10:1 molar ratio Pt:Cd_7MT).

Reaction of K_2PtCl_4 with Cd_7MT under Nitrogen

1.65 mL of 10.5 μM equine kidney Cd_7MT in 3.5 mM phosphate buffer, pH 7.2, was mixed with 0.85 mL of 163 μM K_2PtCl_4 (8:1 molar ratio Pt:Cd7MT) in the glove-box. After 24 hrs the mixture was removed from the glove-box, diluted to 12 mL, concentrated by ultrafiltration, and assayed for S, Cd, and Pt by ICP-AES.

Reaction of K_2PtCl_4 with Native MT under Nitrogen

1 mL of 28 μM native equine kidney MT was mixed with 10 μL of 0.1 M K_2PtCl_4 and allowed to stand for 24 hrs. The products were fractionated on a Sephadex G-50 column. Monomer fractions were pooled and concentrated by ultrafiltration as were fractions consisting of dimers and higher oligomers, and the two resulting solutions assayed for Cd, Zn, Cu, Pt, and S by ICP-AES. A solution of the native MT used in this experiment was also assayed for Cd, Zn, Cu, and S.

Preparation of cis-$Pt(ATMPO)_2Cl_2$

1.00 g K_2PtCl_4 and 0.41 g of 4-amino-2,2,6,6-tetramethylpiperidin-1-oxyl (ATMPO) were dissolved in 25 mL of water and stirred overnight under a slow stream of nitrogen. The brown powder that precipitated, was recrystallized from HCl solution to yield a bright yellow powder. Analytical Calculated: C, 35.52; H, 6.29; N, 9.21. Found: C, 34.25; H, 6.30; N, 8.67.

Preparation of cis-$Pt(NH_3)_2(NO_3)_2$

0.250 g of cis-$Pt(NH_3)_2Cl_2$ was dissolved in 10 mL of water with 0.282 g of $AgNO_3$ and stirred overnight. The AgCl precipitate was removed by passage through a filter paper followed by a 0.2 μm filter. The water was removed in the

lyophilizer and the resulting pale yellow residue used without further purification.

Reaction of cis-$Pt(NH_3)_2(NO_3)_2$ with Native MT

100 µL of a 50 mM cis-$Pt(NH_3)_2(NO_3)_2$ solution in D2O was added to an NMR tube containing 600 µL of a 0.325 mM solution of native rat liver MT-2 buffered at pH 7.2 with 20 mM phosphate. ^1H NMR spectra of the reaction mixture at 25°C were recorded at 10 min intervals for about 2 hrs. After standing 24 hrs the reaction mixture was fractionated on a Sephadex G-50 column. Fractions were pooled, concentrated by ultrafiltration, and assayed for Cd, Zn, Cu, Pt, and S. A sample of the native MT-2 used in this experiment was assayed for Cd, Zn, Cu, and S.

NTSB Disulfide Assay

A 2-nitro-5-thiosulfobenzoate (NTSB) assay solution containing 0.25 mM NTSB and 0.1 M Na_2SO_3 was prepared according to a literature method [172]. Two assays were performed by mixing 0.200 mL of the above solution (pH 9) with 0.500 mL of a 11.7 µM solution of the monomeric products from the reaction of native MT with cis-$Pt(NH_3)_2(NO_3)_2$, and allowing them to react in the dark until the absorbance at 412 nm reached a maximum. The extent of reaction was calculated using the molar absorptivity of the

resulting dianion of 2-nitro-5-thiobenzoic acid, 14150 M^{-1} cm^{-1} at 412 nm [168].

Reaction of cis-$Pt(ATMPO)_2Cl_2$ with Native MT

460 µL of 165 µM cis-$Pt(ATMPO)_2Cl_2$ was mixed with 100 µL of 750 µM native rat liver MT-1 (1:1 molar ratio Pt:MT) in 20 mM Tris/HCl buffer, pH 7.7. After standing for 15 hrs in a 35°C water bath the mixture was fractionated on a Sephadex G-75 column. Fractions were assayed for Cd, Zn, and Pt by high-temperature graphite-furnace atomic absorption spectrometry on a Perkin-Elmer 303 AA spectrometer equipped with a Perkin-Elmer HGA-2000 graphite-furnace. EPR spectra were recorded on a Bruker ER200D Spectrometer for the major protein containing fraction and Pt containing low molecular weight fraction using a quartz flat-cell. The same procedure was performed for a mixture of 460 µL of 165 µM cis-$Pt(ATMPO)_2Cl_2$ with 25 µL of 750 µM native rat liver MT-1 (4:1 molar ratio Pt:MT).

CHAPTER 5
GENERAL CONCLUSIONS

The importance of MT as a major *in vivo* binding site for platinum anticancer drugs is well established [53, 57], but the molecular nature of *in vivo* Pt(II) MT adducts is not known. Concentrations of MT in the cytosol of mammalian cells are on the micromolar level. The experiment in Chapter 4 involving an equimolar mixture of *cis*-$Pt(ATMPO)Cl_2$ and native MT at approximately physiological temperature and pH suggests that *in vivo* binding of Pt drugs to MT may be confined to the met-1 residue. Zn^{2+} is readily displaced from MT by Pt^{2+} however, and higher doses of Pt drugs could lead to binding of Pt(II) to cysteines in the ß cluster region of MT or the formation of cystine disulfides in the presence of dioxygen and other oxidants. MT concentrations in cells can be increased over 100-fold by induction of MT biosynthesis [179] and the elevated levels of MT could also lead to more extensive binding of Pt(II) from Pt drugs to MT.

The Pt-induced oligomerization of MT found for the reactions of K_2PtCl_4 and *cis*-$Pt(NH_3)_2(NO_3)_2$ with native MT should be taken into account when analyzing the distribution of Pt and other metals in size-exclusion chromatographic

profiles of liver and kidney extracts from Pt treated animals. Such oligomeric MT might very well contribute to the metal contents of high-molecular-weight-fractions attributed to higher MW proteins. Sulfur assays might be a more valid way of identifying the MT-containing fractions than hydrodynamic properties.

It is somewhat surprising that Pt(II) compounds show little or no ability to induce the biosynthesis of MT [57, 58] as induction is most prominent for heavy metal ions with toxicities and type b acceptor properties similar to Pt(II) [180]. The genetic mechanism of MT induction by metal ions is not well understood yet and it is possible that the stereochemistry of the metal ion is important, and in this respect Pt(II) is considerably different from the other metal ions that have been studied.

The experimental results presented in Chapter 4 clearly show that Pt(II) from cisplatin derivatives displaces Zn^{2+} from native MT leaving the more strongly bound Cd^{2+} and Cu^{+} intact. Depletion of available cisplatin by MT in tumor cells could diminish the effectiveness of cancer treatment with this drug [61, 181]. If MT is important in the regulation of Zn levels the binding of Pt(II) to the ß cluster region of MT could also have deleterious effects on the patient by disrupting Zn homeostasis.

On the other hand, sequestering of toxic Pt(II) metabolites by MT could be very beneficial in protecting the

patient from the inactivation of enzymes and other more critically important biomolecules. Naganuma and coworkers [64] have reported that the toxic effects of cisplatin in rats are substantially prevented, following induction of MT biosynthesis by $Bi(NO_3)_3$, without compromising the antitumor activity of cisplatin. $Bi(NO_3)_3$ and other agents may selectively induce biosynthesis of MT in healthy tissue but not in the tumor cells. It is likely that MT plays an important role in the sequestering of Cd^{2+} and other toxic metal ions, and a better understanding of the interactions of MT with metal ions could lead to new treatments for heavy metal poisoning.

REFERENCES

1. Kagi, J. H. R.; Nordberg, M., Eds. Metallothionein; Birkhauser-Verlag: Basel, 1979.

2. Vasak, M.; Kagi, J. H. R. Metal Ions in Biological Systems; Sigel, H., Ed.; Marcel Dekker: New York 1983, 15, 213.

3. Vasak, M. J. Mol. Catalysis 1984, 23, 293.

4. Kagi, J. H. R.; Kojima, Y., Eds. Metallothionein-2; Birkhauser-Verlag: Basel, 1988.

5. Margoshes, M.; Vallee, B. L. J. Am. Chem. Soc. 1957, 235, 4813.

6. Kojima, Y.; Berger, C.; Kagi, J. H. R. Metallothionein; Kagi, J. H. R.; Nordberg, M., Eds.; Birkhauser: Basel, 1979, p. 153.

7. Winge, D. R.; Nielson, K. B.; Zeikus, R. D.; Gray, W. R. J. Biol. Chem. 1984, 259, 11419.

8. Furey, W. F.; Robbins, A. H.; Clancy, L. L.; Winge, D. R.; Wang, B. C.; Stout, C. D. Science 1986, 231, 704.

9. Collett, S. A.; Stout, C. D. Recl. Trav. Chim. Pays-Bas: Proceedings of the Third International Conference on Bioinorganic Chemistry (Noordwijkerhout, Netherlands); van Koten, G.; Reedijk, J., Eds.; Elsevier: Amsterdam, 1987, 106, 182.

10. Kagi, J. H. R. 8th Int. Congr. Biochem. Abstr. 1970, Switzerland, p130.

11. Mehra, R. K.; Bremner, I. Biochem. J. 1984, 219, 539.

12. Szymanska, J. A.; Zelazowski, A. J.; Stillman, M. J. Biochem. Biophys. Res. Comm. 1983, 115, 167.

13. Day, F. A.; Funk, A. E.; Brady, F. O. Chem.-Biol. Interactions **1984**, 50, 159.

14. Funk, A. E.; Day, F. A.; Brady, F. O. Comp. Biochem. Physiol. **1987**, 86C, 1.

15. Ikebuchi, H.; Teshima, R.; Suzuki, K.; Sawada, J.; Terao, T.; Yamane, Y. Biochem. Biophys. Res. Comm. **1986**, 136, 535.

16. Schmitz, G.; Minkel, D. T.; Gingrich, D.; Shaw, C. F. III J. Inorg. Biochem. **1980**, 12, 293.

17. Szymanska, J. A.; Stillman, M. J. Biochem. Biophys. Res. Comm. **1982**, 108, 919.

18. Zelazowski, A. J.; Garvey, J. S.; Hoeschele, J. D. Arch. Biochem. Biophys. **1984**, 229, 246.

19. Otvos, J. D.; Engeseth, H. R.; Wehrli, S. Biochemistry **1985**, 24, 6735.

20. Nettesheim, D. G.; Engeseth, H. R.; Otvos, J. D. Biochemistry **1985**, 24, 6744.

21. Stillman, M. J.; Cai, W.; Zelazowski, A. J. J. Biol. Chem. **1987**, 262, 4538.

22. Stillman, M. J.; Zelazowski, A. J. J. Biol.Chem. **1988**, 263, 6128.

23. Vasak, M.; Worgotter, E.; Wagner, G.; Kagi, J. H. R.; Wuthrich, K. J. Mol. Biol. **1987**, 196, 711.

24. Szymanska, J. A.; Law, A. Y. C.; Stillman, M. J.; Zelazowski, A. J. Inorg. Chim. Acta **1983**, 79, 123.

25. Johnson, B. A.; Armitage, I. M. Inorg. Chem. **1987**, 26, 3139.

26. Laib, J. E.; Shaw, C. F. III; Petering, D. H.; Eidsness, M. K.; Elder, R. C.; Garvey, J. S. Biochemistry **1985**, 24, 1977.

27. Bongers, J.; Bell, J. U.; Richardson, D. E. J. Inorg. Biochem. **1988** , 34, 55.

28. Waalkes, M. P.; Harvey, M. J.; Klaassen, C. D. Toxicology Letters **1984**, 20, 33.

29. Vasak, M.; Kagi, J. H. R.; Holmquist, B.; Vallee, B. L. Biochemistry **1981**, 20, 6659.

30. Vasak, M. J. Am. Chem. Soc. **1980**, 102, 3953.

31. Good, M.; Vasak, M. Biochemistry **1986**, 25, 8353.

32. Nielson, K. B.; Winge, D. R. J. Biol. Chem. **1984**, 259, 4941.

33. Byrd, J.; Winge, D. R. Arch. Biochem. Biophys. **1986**, 250, 233.

34. George, G. N.; Winge, D.; Stout, C. D.; Cramer, S. P. J. Inorg. Biochem. **1986**, 27, 213.

35. Nielson, K. B.; Winge, D. R. J. Biol. Chem. **1983**, 258, 13063.

36. Avdeef, A.; Zelazowski, A. J.; Garvey, J. S. Inorg. Chem. **1985**, 24, 1928.

37. Bernhard, W. R.; Vasak, M.; Kagi, J. H. R. Biochemistry **1986**, 25, 1975.

38. Willner, H.; Vasak M.; Kagi, J. H. R. Biochemistry **1987**, 26, 6287.

39. Vasak, M.; Hawkes, G. E.; Nicholson, J. K.; Sadler, P. J. Biochemistry **1985**, 24, 740.

40. Bernhard, W. R.; Good, M.; Vasak, M.; Kagi, J. H. R. Inorg. Chim. Acta **1983**, 79, 154.

41. Nielson, K. B.; Atkin, C. L.; Winge, D. R. J. Biol. Chem. **1985**, 260, 5342.

42. Thomson, A. J.; Williams, R. J. P.; Reslova, S. Structure and Bonding, Springer-Verlag: New York, **1972**, 11, 1.

43. Cisplatin; Current Status and New Developments, Prestayko, A. W.; Crooke, S. T.; Carter, S. K.; Alder, N. A., Eds.; Academic Press: New York, **1980**.

44. Rosenberg, B.; Van Camp, L.; Trosko, J. E., Mansour, V. H. Nature **1969**, 222, 385.

45. Pinto, A. L.; Lippard, S. J. Biochem. Biophys. Acta **1985**, 780, 167.

46. Howe-Grant, M. E.; Lippard, S. J. Metal Ions in Biological Systems; Sigel, H., Ed.; Marcel Dekker: New York, **1980**, 11, 63.

47. Melius, P.; Friedman, M. E. Inorg. Perspect. Biol. Med. 1978, 1, 1.

48. Von Hoff, D. D.; Schilsky, R.; Reichert, C. M.; Reddick, R. L.; Rozencweig, M.; Young, R. C.; Muggia, F. M. Cancer Treat. Rep. 1979, 63, 1527.

49. Hartley, F. R. The Chemistry of Platinum and Palladium; John Wiley and Sons: New York, 1973.

50. Blundell, T. L.; Johnson, L. N. Protein Crystallography; Academic Press: New York, 1976, Chpt. 8.

51. Hoeschele, J. D.; Butler, T.A.; Roberts, J. A. Inorganic Chemistry in Biology and Medicine; Martell, A. E., Ed.; Am. Chem. Soc.: Washington D. C., 1980, p. 181.

52. Robins, A. B.; Leach, M. O. Cancer Treat. Rep. 1983, 67, 245.

53. Litterst, C. L. Agents and Actions 1984, 15, 520.

54. Sharma, R. P.; Edwards, I. R. Biochem. Pharmacol. 1983, 32, 2665.

55. Choie, D. D.; del Campo, A. A.; Guarino, A. M. Tox. Appl. Pharmacol. 1980, 55, 245.

56. Sharma, R. P. Pharmacol. Res. Comm. 1985, 17, 197.

57. Zelazowski, A. J.; Garvey, J. S.; Hoeschele, J. D. Arch. Biochem. Biophys. 1984, 229, 246.

58. Kinsler, S.; Bell, J. U. Biochemistry Int. 1985, 10, 847.

59. Bakka, A.; Endresen, L., Johnsen, A. B. S., Edminson, P. D.; Rugstad, H. E. Toxicol. Appl. Pharmacol. 1981, 61, 215.

60. Endresen, L.; Schjerven, L.; Rugstad, H. E. Acta Pharmacol. et Toxicol. 1984, 55, 183.

61. Kelly, S. L.; Basu, A.; Teicher, B. A.; Hacker, M. P.; Hamer, D. H.; Lazo, J. S. Science 1988, 241, 1813.

62. Naganuma, A.; Satoh, M.; Koyama, Y.; Imura, N. Toxicol Lett. 1985, 24, 203.

63. Satoh, M.; Naganuma, A.; Imura, N. Cancer Chemother. Pharmacol. 1988, 21, 176.

64. Naganuma, A.; Satoh, M., Imura, N. Cancer Res. 1987, 47, 983.

65. Buhler, R. H. O.; Kagi, J. H. R. Metallothionein; Kagi, J. H. R.; Nordberg, M., Eds.; Birkhauser: Basel, 1979, p. 211.

66. Wetlaufer, D. B., Adv. Protein Chem. 1962, 17, 296.

67. Bongers, J.; Walton, C. D.; Richardson, D. E.; Bell, J. U. Anal. Chem., in press.

68. Heine, D. R.; Babis, J. S.; Denton, M. B. Appl. Spectrosc. 1980, 34, 595.

69. Nygaard, D. D.; Leighty, D. A. Appl. Spectrosc. 1985, 39, 968.

70. Suzuki, K. T.; Kobayashi, E.; Sunaga, H.; Shimojo, N. Anal.Lett. 1986, 19, 863.

71. Morita, M.; Uehiro, T.; Fuwa, K. Anal. Chim. Acta 1984, 166, 283.

72. Sunaga, H.; Kobayashi, E.; Shimojo, N.; Suzuki, K. T. Anal.Biochem. 1987, 160, 160.

73. Kojima, Y.; Berger, C.; Vallee, B. L.; Kagi, J. H. R. Proc. Natl. Acad. Sci. 1976, 73, 3413.

74. Vasak, M.; Kagi, J. H. R.; Hill, H. A. O. Biochemistry 1981, 20, 2852.

75. Margoliash, E.; Smith, E. L. Nature 1961, 192, 1125.

76. Myer, Y. P.; MacDonald, L. H.; Verma, B. C.; Pande, A. Biochemistry 1980, 19, 199.

77. Butt, W. D.; Keilin, D. Proc. Roy. Soc. 1962, B156, 429.

78 Margoliash, E. ; Frohwirt, N. Biochem. J. 1959, 71, 570.

79. Kirschenbaum, D. M. Handbook of Biochemistry and MolecularBiology, 3rd ed.; Fasman, G. D., Ed.; CRC Press: Cleveland, 1975; 2, p. 383.

80. Webster, G. C. Biochim. Biophys. Acta **1970**, 207, 371.

81 Mayer, M. M.; Miller, J. A. Anal. Biochem. **1970**, 36, 91.

82. Dautrevaux, M.; Boulanger, Y.; Han, K.; Biserte, G. Eur. J. Biochem. **1969**, 11, 267.

83. Antonini, E.; Brunori, M. Hemoglobin and Myoglobin in their Reactions with Ligands; American Elsevier: New York, **1971**, p. 44.

84. Romberg, R. W.; Kassner, R. J. Biochemistry **1979**, 18, 5387.

85. Antonini, E. Physiol. Rev. **1965**, 45, 123.

86. Rossi-Fanelli, A.; Antonini, E.; Povoledo, D. Symposium on Protein Structure; Neuberger, A., Ed.; Camelot Press Ltd.: London, **1958**; p. 144.

87. Schecter, A. N.; Epstein, C. J. J. Mol. Biol. **1968**, 35, 567.

88. Smyth, D. G.; Stein, W. H.; Moore, S. J. Biol. Chem. **1963**, 238, 227.

89. Meadows, D. H.; Jardetzky, O. Proc. Natl. Acad. Sci. **1968**, 61, 406.

90. Sage, H. J.; Singer, S. J. Biochemistry **1962**, 1, 305.

91. Blumenfeld, O. O.; Levy, M. Arch. Biochem. Biophys. **1958**, 76, 97.

92. Harrington, W. F.; Schellman, J. A. Comptes. Rend. Lab. Carlsberg Ser. Chim. **1956**, 30, 21.

93. Kirschenbaum, D.M. Anal. Biochem. **1975**, 68, 465-484.

94. Krauz, L. M.; Becker, R. R. J. Biol. Chem. **1968**, 243, 4606.

95. Scott, R. A.; Scheraga, H. A. J. Am. Chem. Soc. **1963**, 85, 3866.

96. Tanford, C.; Havenstein, J. D.; Rands, D. G. J. Am. Chem. Soc. **1955**, 77, 6409.

97. Mikes, O.; Holeysovsky, V.; Tomasek, V.; Sorm, F. Biochim. Biophys. Res. Comm. 1966, 24, 346.

98. Maekawa, K.; Leiner, I. E. Arch. Biochem. Biophys. 1960, 91, 108.

99. Kirschenbaum, D.M. Anal. Biochem. 1977, 80, 193.

100. Meloun, B.; Fric, I.; Sorm, F. Eur. J. Biochem. 1968, 4, 112.

101. Green, M. N.; Neurath, H. J. Biol. Chem. 1953, 204, 379.

102. Mihalyi, E.; Harrington, W. F. Biochim. Biophys. Acta 1959, 36, 447.

103. D'Albis, A. Biochim. Biophys. Acta 1970, 200, 34.

104. Jacquot-Armand, Y.; Hill, M. FEBS Lett. 1970, 11, 249.

105. Gentou, C.; Yon, J.; Filitti-Wurmser, S. Bull. Soc. Chim. Biol. 1960, 50, 2003.

106. Green, N. M. Biochem. J. 1957, 66, 407.

107. Buck, F. F.; Vithayathil, A. J.; Bier, M.; Nord, F.F. Arch. Biochem. Biophys. 1962, 97, 417.

108. Schroeder, D. D.; Shaw, E. Arch. Biochem. Biophys. 1971, 142, 340.

109. Robinson, N. C.; Neurath, H.; Walsh, K. A. Biochemistry 1973, 12, 414.

110. Berrens, L.; Bleumink, E. Int. Arch. Allergy 1965, 28, 150.

111. Liu, W.; Trzeciak, H.; Schussler, H.; Meienhoffer, J. Biochemistry 1971, 10, 2849.

112. Abita, J. P.; Delaage, M.; Lazdunski, M.; Savrda, J. Eur. J. Biochem. 1969, 8,314.

113. Blow, D. M.; Birktoft, J. J.; Hartley, B. S. Nature 1969, 221, 337.

114. Eisenberg, M. A.; Schwert, G. W. J. Gen. Physiol. 1951, 34, 583.

115. Nichol, J. C. J. Biol. Chem. 1968, 243, 4065.

116. Brandts, J.; Lumry, R. J. Phys. Chem. 1963, 67, 1484.
117. Wilcox, P. E.; Cohen, E.; Tan, W. J. Biol. Chem. 1957, 228, 999.
118. Chervenka, C. H. Biochim. Biophys. Acta 1959, 31, 85.
119. Jackson, L. M.; Becker, R. R. Biochemistry 1970, 9, 2294.
120. Smillie, L. B.; Enenkel, A. G.; Kay, C. M. J. Biol. Chem. 1966, 241, 2097.
121. Wu, F. C.; Laskowski, M. J. Biol. Chem. 1955, 213, 609.
122. Guy, O.; Gratecos, D.; Rovery, M.; Desnvelle, D. Biochim. Biophys. Acta 1966, 115, 404.
123. Raval, D. N.; Schellman, J. A. Biochim. Biophys. Acta 1965, 107, 463.
124. Myers, S. A.; Tracy, D. H. Spectrochim. Acta 1983, 38B, 1227.
125. Boumans, P. W. J. M. Inductively Coupled Plasma Emission Spectrometry - Part 1: Methodology, Instrumentation, and Performance; Boumans, P. W. J. M., Ed.; Wiley-Interscience: New York, 1987, p. 85.
126. Christian, G. D.; Ruzicka, J. Spectrochim. Acta 1987, 42B, 157.
127. Lawrence, K. E.; Rice, G. W.; Fassel, V. A. Anal. Chem. 1984, 56, 289.
128. Koropchak, J. A.; Winn, D. H. Anal. Chem. 1986, 58, 2558.
129. Lee, J.; Pritchard, M. W. Spectrochim. Acta Biochem. Biotechnol. 1982, 36B, 591.
130. Sobocinski, P. Z.; Canterbury, W. J. Jr.; Mapes, C. A.; Dinterman, D. E. Am. J. Physiol. 1978, 234, E399.
131. Wallace, G. F.; Pirc, V. V.; Ediger, R. D. Can. J. Spectrosc. 1982, 27, 46.
132. McGuinness, E. T. J. Chem. Ed. 1973, 50, 826.

133. Schechter, Y. J. Biol. Chem. **1986**, 261, 66.

134. Kagi, J. H. R.; Himmelhoch, S. R.; Whanger, P. D.; Bethune,J. L.; Vallee, B. L. J. Biol. Chem. **1961**, 236, 2435.

135. Galdes, A.; Hill, H. A. O.; Kagi, J. H. R.; Vasak, M.; Bremner, I.; Young, B. W. Metallothionein; Kagi, J. H. R.; Nordberg, M., Eds.; Birkhauser: Basel, **1979**, p. 241.

136. Takahashi, H.; Nara, Y.; Yoshida, T.; Tuzimura, K.; Meguro, H. Agric. Biol. Chem. **1981**, 45, 79.

137. Vasak, M.; Kagi, J. H. R. Proc. Natl. Acad. Sci. USA **1981**, 78, 6709.

138. Gray, H. B. Transition Metal Chemistry; **1965**, 1, 239.

139. Martin, D. S. Jr.; Rush, R. M.; Peters, T. J. Inorg. Chem. **1976**, 15, 669.

140. Day, P.; Smith, M. J.; Williams, R. J. P. J. Chem. Soc. A. **1968**, 668.

141. Mason, W. R. III; Gray, H. B. J. Am. Chem. Soc. **1968**, 90, 5722.

142. Olsson, L. Inorg. Chem. **1986**, 25, 1697.

143. Kroening, R. F.; Rush, R. F.; Martin, D. S.; Clardy, J. C. Inorg. Chem. **1974**, 13, 1366.

144. Jorgensen, Prog. Inorg. Chem. **1970**, 12, 101.

145. Kozelka, J.; Luthi, H.; Dubler, E.; Kunz, R. W. Inorg. Chim. Acta **1984**, 86, 155.

146. Rawn, D. J. Biochemistry; Harper & Row: New York, **1983**, Chapter 4.

147. Rupp, H.; Weser, U. Biochim. Biophys. Acta **1978**, 533, 209.

148. Pande, J.; Pande, C.; Gilg, D.; Vasak, M., Callender, R.; Kagi, J. H. R. Biochemistry, **1986**, 25, 5526.

149. Otvos, J. D.; Armitage, I. M. J. Am. Chem. Soc. **1979**, 101, 7734.

150. Wagner, G.; Neuhaus, D.; Worgotter, E.; Vasak, M.; Kagi, J. H. R.; Wuthrich, K. Eur. J. Biochem. **1986**, 157, 275.

151. Worgotter, E.; Wagner, G.; Vasak, M.; Kagi, J. H. R.; Wuthrich, K. Eur. J. Biochem. **1987**, 167, 457.

152. Braun, W.; Wagner, G.; Worgotter, E.; Vasak, M.; Kagi, J. H. R.; Wuthrich, K. J. Mol. Biol. **1986**, 187, 125.

153. Wagner, G.; Neuhaus, D.; Worgotter, E.; Vasak, M.; Kagi, J. H. R.; Wuthrich, K. J. Mol. Biol. **1986**, 187, 131.

154. Vasak, M.; Galdes, A.; Hill, H. A. O.; Kagi, J. H. R.; Bremner, I.; Young, B. W. Biochemistry **1980**, 19, 416.

155. Vasak, M.; Berger, C.; Kagi, J. H. R. FEBS Lett. **1984**, 168, 174.

156. Pande, J.; Vasak, M.; Kagi, J. H. R. Biochemistry **1985**, 24, 6717.

157. Vasak, M.; McClelland, C. E.; Hill, H. A. O., Kagi, J. H. R. Experientia **1985**, 41, 30.

158. Mitsumori, F.; Tohyama, C. J. Biochem. **1984**, 96, 533.

159. Campbell, I. D.; Dobson, C. M.; Williams, R. J. P.; Wright, P. E. FEBS Lett. **1975**, 57, 96.

160. Galdes, A.; Vasak, M.; Hill, H. A. O.; Kagi, J. H. R. FEBS Lett. **1978**, 92, 17.

161. Ismail, I. M.; Kerrison, S. J. S.; Sadler, P. J. Polyhedron **1982**, 1, 57.

162. Gummin, D. D.; Ratilla, E. M. A.; Kostic, N. M. Inorg. Chem. **1986**, 25, 2429.

163. Boswell, A. P.; Moore, G. R.; Williams, R. J. P. Biochem J. **1982**, 201, 523.

164. Bell, J. D.; Norman, R. E.; Sadler, P. J. J. Inorg. Biochem. **1987**, 31, 241.

165. Otvos, J. D.; Olafson, R. W.; Armitage, I. M. Biochemical Structure Determination by NMR; Sykes, B. D.; Glickson, J.; Bothner-By, A. A., Eds.; Marcel Dekker: New York, 1981, p. 65.

166. Hunt, C. T.; Boulanger, Y.; Fesik, S. W.; Armitage, I. M. Env. Health Persp. 1984, 54, 135.

167. Ismail, I. M.; Sadler, P. J. Platinum, Gold, and Other Metal Chemotheraputic Agents; A. C. S. Symp. Ser., 1983, 209, 171.

168. Riddles, P. W.; Blakeley, R. L.; Zerner, B. Anal. Biochem. 1979, 94, 75.

169. Carr, H. Y.; Purcell, E. M. Phys. Rev. 1954, 94, 630.

170. Templeton, D. M.; Dean, P. A. W.; Cherian, M. G. Biochem. J. 1986, 234, 685.

171. Briggs, R. W.; Armitage, I. M. J. Biol. Chem. 1982, 257, 1259.

172. Thannhauser, T. W.; Konishi, Y.; Scheraga, H. A. Methods in Enzymology; Jakoby, W. B.; Griffith, O. W., Eds.; Academic Press: Orlando, 1987, 143, 115.

173. Mathew, A.; Bergquist, B.; Zimbrick, J. J. Chem. Soc. Chem. Comm. 1979, 222.

174. Bird, P. H.; Siriwardane, U.; Rabin, D. L.; Shaver, A. Can. J. Chem. 1982, 60, 2075.

175. Gibson, D.; Lippard, S. J. Inorg. Chem. 1986, 25, 219.

176. Dance, I. G. Polyhedron 1986, 5, 1037.

177. Fackler, J. P. Jr.; Zegarski, W. J. J. Am. Chem Soc. 1973, 95, 8566.

178. McPartlin, E. M.; Stephenson, N. C. Acta Cryst. 1969, B25, 1659.

179. Karin, M. Cell 1985, 41, 9.

180. Jones, M. M.; Meredith, M. J.; Dodson, M. L.; Topping, R. J.; Baralt, E. Inorg. Chim. Acta 1988, 153, 87.

181. Andrews, P. A.; Murphy, M. P.; Howell, S. B. Cancer Chemother. Pharmacol. **1987**, 19, 149.

BIOGRAPHICAL SKETCH

Jacob Bongers was born in Milwaukee on February 6, 1959, to Donald and June Bongers. He spent most of his childhood in Green Bay, Wisconsin, where he graduated from South West High School. Jacob attended Macalester College in Saint Paul, Minnesota, for one year. After spending a semester away from school to complete training as a medic for the army national guard, he enrolled at the University of Wisconsin in Green Bay. After receiving his B.S. degree in 1982, he began work towards a doctoral degree in chemistry at the University of Florida, under the supervision of Dr. David E. Richardson. On July 23, 1988, Jacob married Cyndy Walton of London Grove, Pennsylvania, who is also a doctoral candidate in chemistry.

I certify that I have read this study and that in my opinion it conforms to acceptable standards of scholarly presentation and is fully adequate, in scope and quality, as a dissertation for the degree of Doctor of Philosophy.

David E. Richardson, Chairman
Associate Professor of Chemistry

I certify that I have read this study and that in my opinion it conforms to acceptable standards of scholarly presentation and is fully adequate, in scope and quality, as a dissertation for the degree of Doctor of Philosophy.

Paul W. Chun
Professor of Biochemistry and Molecular Biology

I certify that I have read this study and that in my opinion it conforms to acceptable standards of scholarly presentation and is fully adequate, in scope and quality, as a dissertation for the degree of Doctor of Philosophy.

George E. Ryschkewitsch
Professor of Chemistry

I certify that I have read this study and that in my opinion it conforms to acceptable standards of scholarly presentation and is fully adequate, in scope and quality, as a dissertation for the degree of Doctor of Philosophy.

R. Carl Stoufer
Associate Professor of Chemistry

I certify that I have read this study and that in my opinion it conforms to acceptable standards of scholarly presentation and is fully adequate, in scope and quality, as a dissertation for the degree of Doctor of Philosophy.

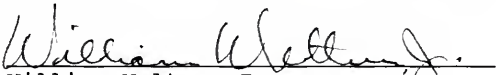

William Weltner Jr.
Professor of Chemistry

This dissertation was submitted to the Graduate Faculty of the Department of Chemistry in the College of Liberal Arts and Sciences and to the Graduate School and was accepted as partial fulfillment of the requirements for the degree of Doctor of Philosophy.

May, 1989

_____
Dean, Graduate School

UNIVERSITY OF FLORIDA
3 1262 08553 4583